Hippocampus-lateral septum circuitry mediates foraging-related spatial memory in rats

Elizabeth A. Davis[1]*, Clarissa M. Liu[1,2]*, Isabella H. Gianatiempo[1], Andrea N. Suarez[1], Alyssa M. Cortella[1], Joel D. Hahn[3], and Scott E. Kanoski[1,2]

*These two authors contributed equally
[1]Human and Evolutionary Biology Section, Department of Biological Sciences, Dornsife College of Letters, Arts and Sciences, University of Southern California, 3616 Trousdale Pkwy, Los Angeles, CA, USA, 90089; [2]Neuroscience Graduate Program, University of Southern California, 3641Watt Way, Los Angeles, CA, USA. 90089; [3]Neurobiology Section, Department of Biological Sciences, Dornsife College of Letters, Arts and Sciences, University of Southern California, 3616 Trousdale Pkwy, Los Angeles, CA, USA, 90089

Corresponding author:
Scott E. Kanoski, PhD
University of Southern California
3616 Trousdale Parkway, AHF-252
Los Angeles, CA 90089-0372
Phone: 213-821-5762
Email: kanoski@usc.edu

Classification: Biological Sciences, Neuroscience

Keywords: feeding, cognition, place cells, motivation, reward, foraging, lateral hypothalamic area, prefrontal cortex

1   **ABSTRACT**

2

3   Remembering the location of a food or water source is essential for survival. Here we

4   identify a hippocampal-septal neural circuit that is necessary for spatial memory based

5   specifically on appetitive reinforcement. Both reversible and chronic disconnection of ventral

6   hippocampus CA1 subregion (CA1v) projections to the lateral-septum (LS) using pathway-

7   specific dual viral approaches impaired spatial memory retention for the location of either food

8   or water reinforcement. However, disconnection of this pathway did not affect performance in an

9   aversive escape-motivated spatial memory task that used the same apparatus and visuospatial

10 cues. The selectivity of this pathway in mediating foraging-related spatial memory was further

11 supported by results showing that CA1v-LS disconnection did not affect anxiety-like behavior,

12 locomotor activity, or social and olfactory-based appetitive learning. To examine whether CA1v-

13 LS mediation of foraging-related spatial memory involves collateral projections of CA1v

14 neurons, we utilized virus-based neural pathway tracing analyses to identify the medial

15 prefrontal cortex (mPFC) as a collateral target of LS-projecting CA1v neurons. However,

16 functional disconnection of CA1v and mPFC did not affect appetitive spatial memory, thus

17 further supporting the selectivity of CA1v-LS signaling for this behavior. The nucleus

18 accumbens, lateral hypothalamic area, and other brain regions associated with food motivation

19 and reward were identified as second-order targets of CA1v-LS signaling using a multisynaptic

20 anterograde tracing approach. Collective results reveal that CA1v to LS communication plays a

21 critical role in remembering an environmental location based on appetitive (food or water) but

22 not aversive (escape) reinforcement, thus identifying a novel neural pathway regulating foraging-

23 related memory processes.

24

25

26

27

28

29

30

31

32

INTRODUCTION

34

35   A survival advantage common to early humans and lower-order mammals is to accurately

36   remember the location of a food or water source in the environment, and to then efficiently

37   navigate back to a shelter or other safe location. The neurobiological substrates that regulate

38   visuospatial navigation are therefore critical to effectively implement food-directed or water-

39   directed foraging behavior. In rodents a number of maze tasks have been developed for studying

40   spatial memory and navigation, including the widely popular Morris water maze that requires

41   animals to swim and navigate to a submerged escape platform using distal viusospatial cues as a

42   guide (1). The conceptually similar Barnes maze task requires animals to learn and recall a

43   location for escaping mildly aversive stimuli (bright lights, loud noises) (2). These and other

44   tasks have been instrumental in identifying brain structures within the telencephalon that are

45   essential for visuospatial mapping and egocentric orientation in the environment, including the

46   hippocampus and the medial entorhinal cortex, respectively (3, 4). However, despite that reliably

47   locating food and water sources in the environment is a key selection pressure driving evolution

48   of visuospatial navigation, the overwhelming majority of rodent model research on the substrates

49   of spatial learning and memory have utilized procedures such as the Morris water maze and the

50   Barnes maze that each involve escaping aversive reinforcement (5, 6). Furthermore, while single

51   unit recordings have been used to identify specific populations of neurons that subserve distinct

52   navigational functions (e.g., hippocampal "place cells", medial entorhinal "grid cells") (7, 8), the

53   bulk of this research has recorded neural activity under neutral conditions void of either

54   appetitive or aversive reinforcement. Very little research has been dedicated to identify brain

55   regions and neural circuits that may specifically promote spatial memory based on the location of

56   appetitive reinforcers (e.g., food, water), as well as the extent to which the nature of the

57   reinforcement is a critical factor in deciphering the brain's control of visuospatial navigation.

58   The majority of rodent model research investigating brain regions that mediate

59   visuospatial navigational memory has focused on the anterior and "dorsal" subregion of the

60   hippocampus (septal pole; HPCd). However, the posterior and "ventral" hippocampus subregion

61   (temporal pole; HPCv), while classically associated with stress- and affect-associated memory

62   processes (9), also plays a role in visuospatial learning and memory (10-12). For example, under

63   some testing conditions selective HPCv lesions impair spatial memory performance in the Morris

64   water maze (12, 13). Moreover, place cells that are responsive to changes in the visuospatial

65   environment are present within both the HPCd and HPCv pyramidal layers, with a linear

66   increase in the scale of representation from the dorsal to the ventral pole (11). Despite a common

67   role for the HPCd and HPCv in mediating spatial memory, there is also evidence for a functional

68   distinction between the subregions (9, 14, 15). For instance, lesions of the HPCv but not the

69   HPCd alter stress responses (16) and anxiety-like behavior (17), whereas HPCd but not HPCv

70   lesions impair spatial memory in an incidental (nonreinforced) procedure (18). These two HPC

71   subregions also have distinct afferent and efferent neural connections. This disparate

72   neuroanatomical connectivity supports a framework for a functional diversity in which the HPCd

73   preferentially processes cortical-derived sensory information and the HPCv preferentially

74   processes metabolic and limbic-derived affective information (9, 15). The functional distinction

75   between these two subregions is further supported by the generation of the hippocampus gene

76   expression atlas, which provides a comprehensive integration of gene expression and

77   connectivity across the HPC axis (19). Given that both the HPCv and the HPCd participate in

78   spatial memory but have distinct neuroanatomical connectivity and contributions when it comes

79   to regulating other cognitive and mnemonic processes, it is feasible that the HPCv and HPCd

80   support different forms of spatial memory depending on the type of reinforcement and/or the

81   context associated with the behavior.

82   Recent findings identify the HPCv as a critical brain substrate in regulating feeding

83   behavior and food-directed memory processes. Reversible inactivation of HPCv neurons after a

84   meal increases the size of and reduces the latency to consume a subsequent meal (20, 21). In

85   addition, receptors for feeding-related hormones are more abundantly expressed in the HPCv

86   compared to the HPCd (e.g., ghrelin receptors (22, 23), glucagon-like peptide-1 [GLP-1]

87   receptors (24)), and these HPCv endocrine and neuropeptide receptor systems alter food intake

88   and feeding-related memory (25). For example, leptin and GLP-1 act in the HPCv (CA1v

89   subregion) to decrease food intake and food-motivated conditioned behaviors (26-28), whereas

90   the orexigenic gut-derived hormone ghrelin administered to the HPCv but not HPCd has

91   opposite effects (25, 29). Olfactory information, which is intimately connected with feeding

92   behavior, is also preferentially processed within the HPCv compared with the HPCd. The CA1v,

93   specifically, is bidirectionally connected to brain regions that process olfactory information (9,

94   30, 31), and CA1v neurons respond more robustly to olfactory contextual cues compared with

95   CA1d (10). Further, ghrelin signaling in the CA1v improves olfactory- and socially-mediated

96   memory for food preference (32). Given the HPCv appetite-relevant neuroanatomical

97   connections, endocrine and neuropeptide receptor expression profiles, and functional evidence

98   linking this subregion with food-motivated behaviors, we hypothesize that HPCv mediation of

99   visuospatial memory is preferentially biased to food and water-reinforced foraging behavior.

100   HPCv pyramidal neurons have extensive projection targets throughout the brain (33), yet

101   the functional relevance of these pathways is poorly understood. Recently, CA1v projections to

102   the medial prefrontal cortex (mPFC) and lateral hypothalamic area (LHA) were found to mediate

103   feeding-related outcomes associated with GLP-1 and ghrelin signaling, respectively (28, 34).

104   CA1v neurons also robustly target the LS (35, 36), and a HPCv dentate gyrus-CA3v to lateral

105   septum (LS) pathway was identified that suppresses feeding (37). However, the relevance of this

106   pathway to feeding-related learning and memory is unknown. It is feasible that CA1v to LS

107   projections participate in regulating spatial memory for food location, a notion supported by

108   findings showing that neuroplastic changes occur in the LS after learning a spatial memory task

109   (38, 39). Thus, in addition to exploring the role of the HPCv in memory for the spatial location

110   of food or water, the present study also investigated the specific role of the CA1v to LS pathway

111   in foraging-relevant memory processes.

112   To systematically investigate the role of the HPCv and CA1v to LS signaling in

113   visuospatial learning and memory for food and water reinforcement, we developed two novel

114   appetitive reinforcement-based spatial foraging behavioral tasks that allows for direct

115   comparison with an aversive reinforcement-based task of similar difficulty that uses the same

116   apparatus and spatial cues. Performance in these tasks was assessed following pathway-specific

117   dual viral-based reversible (chemogenetic inhibition) or chronic (targeted apoptosis)

118   disconnection of the CA1v to LS pathway. To further expand neural network knowledge on

119   CA1v to LS signaling, we used conditional viral-based neuroanatomical tracing strategies to

120   identify both first-order collateral and second-order targets of LS-projecting CA1v neurons.

121   Collective results from the present study identify novel neural circuitry of specific relevance to

122   foraging behavior.

123

124   **RESULTS**

5

125

The ventral hippocampus (HPCv) is required for remembering the spatial location of food

126 **The ventral hippocampus (HPCv) is required for remembering the spatial location of food**

127 To examine the importance of the HPCv in memory for the spatial location of food, animals

128 received bilateral *N*-Methyl-D-aspartate excitotoxic lesions of the HPCv (HPCv lesion n=12) or

129 bilateral sham injections (control n=12) (histological analyses for the neuron-specific NeuN

130 antigen in Fig. 1A) and were tested in a novel appetitive visuospatial memory task developed in

131 our lab. Results revealed no significant differences in errors (incorrect hole investigations) (Fig.

132 1E) or latency to locate the food source hole (Fig. 1F) during training. However, memory probe

133 results show that animals with HPCv lesions decreased the ratio of correct + adjacent / total holes

134 explored in the first minute compared with controls (Figure 1G; p<0.05, cohen's d=-1.0174).

135 Analysis for the combined 2-minute period did not yield a statistical difference between groups.

136 Post-surgical analyses of food intake (Supp. Fig. 1A) and body weight (Supp. Fig. 1B)

137 found no group differences in these measures over time. These collective results indicate the

138 HPCv is required for memory retention but not learning of the spatial location of food in the

139 environment.

140

141 **Ventral hippocampus CA1 (CA1v) projections to the lateral septum (LS) mediate**

142 **appetitive spatial memory for food and water location, but not aversive spatial memory for**

143 **escape location**

144 A major neuroanatomical target of HPCv CA1 neurons (CA1v) is the LS (36). We investigated

145 the functional relevance of the CA1v to LS signaling in learning and recalling the spatial location

146 of either food or water reinforcement using conditional dual viral approaches to either reversibly

147 (via cre-dependent pathway-specific inhibitory chemogenetics; diagram of approach in Fig. 2A)

148 or permanently (via cre-dependent pathway-specific caspase-induced lesions; diagram of

149 approach in Fig. 2B) disconnect CA1v to LS communication. Results from the appetitive food

150 seeking spatial memory task reveal no significant group differences during training in either

151 errors before locating the correct hole (Fig. 2E) or latency to locate the food source hole (Fig.

152 2F). However, memory probe results demonstrate that both acute (pathway-specific DREADDs)

153 and chronic (pathway-specific caspase) CA1v to LS disconnection decreased the ratio of correct

154 + adjacent / total holes explored in the entire two minutes of the probe compared with controls

155   (Fig. 2G; $p<0.05$, cohen's d=-1.142), with a similar trend in the first minute of the probe

156   (p=0.059).

157   Results from the appetitive water seeking spatial memory task in a separate cohort of rats

158   also reveal no significant group differences during training in either errors before locating the

159   correct hole (Fig. 2H) or latency to locate the food source hole (Fig. 2I). However, a significant

160   impairment following either acute or chronic CA1v to LS disconnection of ratio of correct +

161   adjacent / total holes explored in 2-min memory probe compared with controls (Fig 2J; $p<0.05$,

162   cohen's d=-1.18). Analysis for the first minute alone of the probe test did not yield a statistical

163   difference between groups.

164   Histological analyses confirmed successful viral transfection of LS-projecting CA1v

165   neurons with DREADDs (Figs. 2C&D) or caspase (Supp. Figs. 2E&F), and post-surgical

166   analyses of food intake (Supp. Fig 2A) and body weight (Supp. Fig 2B) found no group

167   differences in these measures over time (in the absence of CNO treatment). These data

168   demonstrate that CA1v to LS communication is critical for remembering the spatial location of

169   food and water, and that these effects are unlikely to be based on differences in energy status or

170   food motivation.

171   To evaluate whether the CA1v to LS pathway is specifically involved in appetitive

172   reinforcement-based spatial memory (food or water) vs. spatial memory in general, in a separate

173   cohort of animals we tested the effect of reversible and chronic CA1v to LS disconnection in a

174   spatial learning task based on aversive reinforcement rather than food. Importantly, this task uses

175   the same apparatus and visuospatial cues as the spatial location food and water memory tasks

176   described above, but the animals are motivated to locate the tunnel to escape mildly aversive

177   stimuli (bright lights, loud noise) with no food or water reinforcement in the tunnel (see Fig. 1B).

178   Training results revealed no significant group differences in errors before correct hole (Fig. 2K)

179   nor latency to locate the escape hole (Fig. 2L). During the memory probe test, there were no

180   group differences in the ratio of correct + adjacent / total holes investigated during the first

181   minute nor the entire two minutes (Fig. 2M) of the memory probe. Histological analyses

182   confirmed successful viral transfection of LS-projecting CA1v neurons with DREADDs (Figs.

183   2C&D) or caspase (Supp. Figs. 2E&F), and post-surgical analyses of food intake (Supp. Fig. 2C)

184   and body weight (Supp. Fig. 2D) found no group differences in these measures over time (in the

185   absence of CNO treatment). These collective findings suggest that CA1v to LS signaling

186   specifically mediates spatial memory in a reinforcement-dependent manner, playing a role in

187   appetitive (food or water reward) but not aversive (escape-based) spatial memory.

188

189   **Reversible, but not chronic disconnection of CA1v to LS signaling increases chow intake**

190   **under free-feeding conditions.**

191   While the results above suggest that the impairments in food or water-based spatial

192   memory were not based on long-term changes in food intake or body weight, these experiments

193   were conducted under conditions of either chronic food or water restriction. To examine the role

194   of CA1v to LS signaling on feeding behavior under free-feeding conditions, we examined meal

195   pattern feeding analyses in the caspase vs. the control group (chronic CA1v-LS disconnection),

196   and in the DREADDs group following CNO or vehicle (within-subjects design; reversible

197   CA1v-LS disconnection). Results averaged over 5d revealed no significant effect of chronic

198   CA1v to LS disconnection (caspase group) on 24h meal frequency, meal size, meal duration, or

199   24h food intake in comparison to controls (Supp. Figs. 3A-D). However, acute and reversible

200   silencing of LS-projecting CA1v neurons (DREADDs group; via lateral ventricular injection of

201   the DREADD ligand CNO) significantly increased 24h chow intake (Supp. Fig. 3H; $p<0.05$,

202   cohen's d=0.10) relative to vehicle treatment, accompanied by a trend towards increased meal

203   frequency (Supp. Fig. 3E; p=0.11) and no effect on meal size or meal duration (Supp. Figs.

204   3F&G). These results are unlikely based on nonselective effects of the CNO, as we've recently

205   shown that ICV CNO injections do not affect food intake in rats when tested under similar

206   conditions (40). Collectively these findings show that reversible CA1v to LS disconnection

207   increases food intake under free-feeding conditions, whereas food intake is not affected by

208   chronic CA1v to LS ablation.

209

210   **CA1v to LS disconnection does not affect nonspatial HPC-dependent appetitive memory**

211   To examine the role of CA1v to LS signaling in a nonspatial HPC-dependent food-

212   reinforced memory task, we tested the effect of reversible and chronic CA1v to LS disconnection

213   in the social transmission of food preference (STFP) test (diagram in Fig. 3A). The HPCv plays

214   an important role in STFP (32, 41, 42), which tests socially-mediated food-related memory based

215   on previous exposure to socially-communicated olfactory cues. Results revealed that there were

216   no differences in preference ratio between groups (Fig. 3B), with all three groups performing

8

217 significantly above chance (ps<0.05). These results suggest that neither acute nor chronic CA1v

218 to LS disconnection impair food-related memory based on social-based olfactory stimuli.

219

220 **CA1v to LS disconnection does not affect anxiety-like behavior or levels of locomotor**

221 **activity**

222 HPCv to LS circuitry has been shown to play a role in mediating anxiety and stress behavior (43-

223 45). Given that altered anxiety-like behavior and/or locomotion could produce behavioral

224 changes that may lead to an apparent spatial memory deficit in any of the spatial learning tasks

225 used, we examined whether HPCv to LS disconnection yields differences in anxiety-like

226 behavior (zero maze task; diagram of apparatus in Fig. 3C) and/or locomotion (open field test).

227 Results showed no significant group differences in time spent in the open zones in the zero maze

228 test (Fig. 3D) nor in the number of open zone entries (Fig. 3E), suggesting that neither chronic

229 nor reversible disconnection of the CA1v to LS circuitry influences anxiety-like behavior. In

230 addition, CA1v to LS disconnection had no effect on general locomotor activity in the open field

231 test (Fig. 3F). These results support that observed deficits in food-seeking and water-seeking

232 spatial memory are not secondary to general differences in anxiety-like behavior or locomotor

233 impairments in the disconnection groups.

234

235 **The medial prefrontal cortex is a collateral target of LS-projecting CA1v neurons**

236   In addition to the LS, CA1v neurons also robustly project to the medial prefrontal cortex

237 (mPFC) and the lateral hypothalamic area, two pathways that we have previously shown to be

238 involved in feeding behavior (27, 29, 34). To examine whether LS-projecting CA1v neurons

239 have collateral targets in the mPFC, LHA, or in other brain regions, we utilized a conditional

240 dual viral neural pathway tracing approach that identifies collateral targets of a specific

241 monosynaptic pathway (CA1v->LS; diagram of approach in Fig. 4A, representative CA1v

242 injection site in Fig. 4B, representative CA1v injection site in Fig. 4C). Results revealed that LS-

243 projecting CA1v neurons also project to the mPFC (Fig. 4D), whereas no labeling was observed

244 in the LHA, and very minimal labeling was observed in other brain regions. Thus, it may be the

245 case that the impaired spatial memory for food location observed following either reversible or

246 chronic CA1v to LS disconnection are based, in part, on CA1v to mPFC signaling from the same

247 CA1v to LS projecting neurons.

248

Neither CA1v to mPFC nor CA1v to LHA signaling contribute to spatial memory for food location

We next sought to test the functional relevance to food-directed spatial memory of CA1v-originating neural pathways that either do (CA1v to mPFC) or do not (CA1v to LHA) collateralize from CA1 to LS projections. We also investigated the role of a pathway (CA1v to LHA) that is not a target of LS-projecting CA1v neurons, but has previously been associated with appetitive and consummatory aspects of feeding behavior (29, 34). Both the CA1v to mPFC and CA1v to LHA projections are exclusively ipsilateral (27, 34), and thus these pathways allow for a 'contralesional' approach to achieve chronic functional disconnection (diagram of approach in Fig. 4E&4I, modified from (34)). This approach was utilized in favor of the dual viral approaches used for the CA1v-LS disconnection as it does not require the use of viruses and involves fewer surgical injections to achieve a similar goal. We note that this contralesional approach is not a feasible option for the CA1v-LS pathway, as CA1v neurons project to the LS bilaterally (e.g., Fig. 5F). Post-surgical analyses of food intake (Supp. Fig. 3A,C) and body weight (Supp. Fig. 3B,D) found no group differences in these measures over time for either the CA1v-mPFC or the CA1v-LHA disconnection groups. Training results from the appetitive spatial memory task revealed no group differences in errors before locating the correct hole (Fig. 4F, 4J) or latency to locate the food-baited hole (Fig. 4G, 4K) for either the CA1v-mPFC or the CA1v-LHA disconnection groups. Importantly, memory probe results demonstrate that neither CA1v to mPFC nor CA1v to LHA disconnection altered the ratio of correct + adjacent / total holes explored in the first minute or the entire two minutes (Fig. 4H, 4L) compared with controls. These data collectively demonstrate that CA1v to LS mediation of foraging-related memory does not require collateral projections to the mPFC neural pathway. Further, CA1v to LHA neural signaling, which participates in other conditioned aspects of food intake (29, 34), is not required for either learning or remembering of the spatial location of food.

Second-order targets of CA1v to LS neurons include the mPFC, the LHA, and the ACB

We used a dual viral tracing strategy (diagram of approach in Fig. 5A; representative LS injection site in Fig. 5B) to identify downstream targets of LS-projecting CA1v neurons. Results revealed that the mPFC (Fig. 5C), the LHA (Fig. 5D) and the nucleus accumbens (ACB; Fig. 5E)

10

279 are among the strongest second-order targets of the CA1v to LS-projecting neurons. Quantitative

280 analyses using a custom-built data-entry platform (Axiome C, created by JDH) are summarized

281 graphically for a representative animal on a brain flatmap summary diagram (Fig. 5F) for the

282 hemisphere ipsilateral (top) and contralateral (bottom) to the injection sites. The data are also

283 summarized in tabular form in Supplementary Table 1.

284

285 **DISCUSSION**

286 Memory for the physical location of a food or water source is adaptive for maintaining

287 adequate energy supply for reproduction and survival. However, the neural circuits mediating

288 this complex behavior are not well understood, as research on visuospatial memory has

289 predominantly used tasks with either aversive or neutral/passive reinforcement. Moreover,

290 whether the neural circuitry mediating spatial memory function is divergent based on the nature

291 (e.g., appetitive vs. aversive) or modality (e.g., food vs. water) of the reinforcement has not been

292 systematically investigated. The present study identified a monosynaptic CA1v to LS pathway as

293 a necessary substrate for food- and water-motivated spatial memory. Moreover, the selectivity of

294 the CA1v-LS pathway in mediating spatial memory for food and water location is supported by

295 results showing that disconnection of this pathway did not affect performance in an escape-

296 motivated spatial memory task of comparable difficulty conducted in the same apparatus,

297 anxiety-like behavior, locomotor activity, or olfactory and social-based appetitive memory. Viral

298 pathway tracing identified that LS-projecting CA1v neurons also send collateral projections to

299 the mPFC, however, functional disconnection of CA1v-mPFC signaling did not impair spatial

300 memory for food location. Utilization of an anterograde multisynaptic viral tracing approach and

301 quantitative forebrain-wide axon mapping analyses revealed that the CA1v-LS pathway sends

302 second-order projections to various feeding and reward-relevant neural substrates such as the

303 LHA, ACB, and mPFC. Collectively, these data establish monosynaptic CA1v to LS signaling as

304 essential for spatial memory-based foraging behavior, and we further identify a neural network

305 of interconnected feeding-relevant substrates that are collateral and/or downstream targets of this

306 pathway.

307 Historically, the hippocampus has been divided into the dorsal and ventral subregions

308 that have both distinct and overlapping functions, anatomical connections, and genetic and

309 receptor expression profiles (14, 15, 19, 33, 46). The HPCd has been predominantly implicated

11

310   in facilitating spatial memory, whereas the HPCv is linked with stress responses, affective

311   behavior, and energy balance. However, the HPCv also plays a role in spatial memory,

312   particularly for goal-directed navigation. Consistent with present results, a recent study found

313   that both the HPCd and HPCv were critical for food reward-directed spatial navigation in an

314   obstacle-rich complex environment (47). Under certain testing conditions, spatial learning and

315   memory in an aversive reinforcement-based water maze also requires both subregions of the

316   HPC (48). Similarly, whole-brain analysis of blood flow in rats during retrieval of spatial

317   memory in an aversive reinforcement-based Barnes maze task revealed increased activation in

318   the CA1d and CA1-3v in trained animals compared with controls (49). These results indicate that

319   spatial processing in the hippocampus is organized longitudinally, and that both HPCd and HPCv

320   are important for goal-directed spatial navigation. Here we expand this literature by identifying a

321   specific HPCv-originating pathway (CA1v->LS) that selectively mediates spatial memory for the

322   location of appetitive (food or water) reinforcement.

323   While HPCv neurons project widely throughout the neuraxis, projections to the LS are

324   particularly robust (36). The LS has been implicated in food anticipatory/seeking behavior,

325   where metabolic activation of the lateral septum peaks immediately before feeding (during food

326   anticipatory activity) in rabbit pups (50) and gamma-rhythmic input to the LHA from the LS

327   evokes food approach behavior (51). In addition, the LS can bidirectionally modulate food intake

328   via a number of feeding-relevant neuropeptides, including glucagon-like peptide-1, ghrelin, and

329   urocortin (52-54). A recent finding demonstrated that DREADDs-mediated disconnection of a

330   HPCv to LS pathway (from CA3v and DGv) increases food intake in mice, with

331   opposite/hyperphagic effects observed following activation of this pathway (37). Similarly, here

332   we demonstrate that DREADDs-mediated acute silencing of the CA1v to LS pathway increases

333   food intake in rats. Together these findings support a role for HPCv-LS signaling in regulating

334   feeding behavior. However, these results are based on analyses conducted in the home cage

335   where animals have free and unlimited access to food and water. Here we extend these findings

336   by examining the role of CA1v to LS signaling in foraging-relevant memory processes under

337   conditions that are more relevant to normal mammalian behavior, where food and water are not

338   freely available. Not only do our results identify a novel role for CA1v to LS signaling in

339   processing spatial memory for food and water reward location, but we further show that this

340   circuit appears to selectively promote spatial memory based on appetitive and not aversive-based

341   reinforcement.

342   The use of two different but complementary approaches for neural pathway-specific

343   disconnection allowed us to test at the levels of learning and memory separately. For example,

344   the use of a reversible (DREADDs) disconnection procedure allowed us to evaluate the effect of

345   CA1v to LS disconnection during the memory probe only, with circuit intact during training

346   (CNO was not administered at any point during training). In contrast, the chronic (caspase)

347   disconnection procedure was performed before training and therefore could have affected

348   learning if CA1v to LS pathways were required for the learning of the task. However, our results

349   showed that CA1v to LS did not impair learning, but rather, only memory retention performance

350   in the probe test conducted days after the end of training. Thus, we can now confirm based on

351   two complementary levels of analysis that this pathway is involved in longer-term memory recall

352   but not learning/acquisition, which is consistent with recent evidence demonstrating that

353   complete HPCv lesions impair retrieval (probe performance), but not acquisition (learning) in a

354   Morris water maze (55).

355   Present results identify the CA1v-LS pathway in coordinating reward-motivated behavior

356   with learned spatial information. While the use of aversive reinforcement-based spatial memory

357   tasks are predominant, the radial arm maze has also been used to investigate food-motivated

358   spatial memory (56). Specifically, the radial arm maze examines different components of spatial

359   memory relevant to different foraging strategies. In win-shift tasks, animals learn to avoid

360   previously visited reward arms, which models spontaneous alternation and exploration in

361   environments with minimal resources. On the other hand, in win-stay tasks, animals learn to

362   return to previously reinforced arms modeling foraging in environments of plentiful resources.

363   An advantage of the present food-reinforced Barnes maze approach over the radial arm maze

364   procedure is that we've developed parallel procedures that use the same apparatus and

365   visuospatial cues to examine water- and escape-motivated spatial memory, thus offering a

366   powerful approach to assess the selectivity of the circuit based on multiple reinforcement

367   modalities (food vs. water vs. escape/aversive). While our results clearly support a role for the

368   HPCv in food-reinforced spatial memory, a previous study utilizing a four-baited/four-unbaited

369   version of the eight-arm radial maze task found that NMDA-mediated lesions of the HPCd, but

370   not HPCv, impair spatial reference and working memory (57). Another study using a similar

371   procedure reported that complete HPC lesions impaired both spatial and working memory,

372   whereas lesions to either the HPCd, HPCv, or intermediate HPC had minimal effect on memory

373   performance (58). Future studies will needed to address whether discrepancies between the

374   present results and these studies are based on the differences between the behavioral tasks and/or

375   differences in loss of function methodologies. With regards to the latter, we note that our

376   pathway-specific chemogenetic and caspase-lesion approaches offered far greater specificity

377   (LS-projecting CA1v neurons vs. whole HPCv) compared with these studies.

378   Utilizing dual viral approaches and systematic forebrain-wide quantitative mapping

379   analyses, our findings confirm that the CA1v-LS pathway projects downstream to other neural

380   substrates involved in feeding and motivated behavior, including the LHA, ACB, and mPFC.

381   This experiment was performed to generate novel neural connectivity data for the field and to

382   demonstrate possible downstream 2_{nd}-order targets that may inspire future research on these

383   newly-identified multi-order neural circuits. Given that metabolic activity in the LS and ACB is

384   associated with food anticipatory activity in rabbit pups (50), it is possible that the ACB is a

385   functional downstream target of CA1v-LS signaling for coordinating foraging behavior. It is less

386   likely, however, that the mPFC or the LHA are functional targets of CA1v-LS signaling for

387   appetitive spatial memory control based on the lack of effects on spatial memory for food

388   location when these pathways were disconnected. It is possible, however, that CA1v → LS →

389   mPFC (or → LHA) signaling is relevant to other mnemonic process, such as those involved in

390   drug-motivated or social-based memory tasks.

391   Collective results identify a CA1v to LS pathway involved in food- and water-motivated

392   spatial memory, but not escape-motivated spatial memory. Furthermore, the selectivity of this

393   pathway to appetitive spatial memory is supported by data showing that neither chronic nor

394   reversible disruption of CA1v to LS signaling influenced various other behavioral outcomes,

395   including anxiety-like behavior, locomotor activity, and nonspatial HPC-dependent appetitive

396   memory. We also systematically characterized collateral and second-order projections of this

397   pathway. Present results demonstrate overlapping pathways coordinated in the higher-order

398   control of energy balance, of which foraging behavior is an essential component, given that

399   foraging requires energy expenditure to locate food for subsequent energy intake. These data

400   shed light on the neural systems underlying complex learned and motivated behaviors that

401   require functional connections between cognitive and feeding-relevant substrates.

402

METHODS

404

Animals

406   Adult male Sprague–Dawley rats (Envigo; 250-275g on arrival) were individually housed

407   in hanging wire cages with *ad libitum* access (except where noted) to water and chow (LabDiet

408   5001, LabDiet, St. Louis, MO) on a 12h:12h reverse light/dark cycle. All procedures were

409   approved by the University of Southern California Institute of Animal Care and Use Committee.

410

General intracranial injection procedures

412   Rats were anesthetized via an intramuscular injection of an anesthesia cocktail (ketamine

413   90mg/kg body weight [BW], xylazine, 2.8mg/kg BW and acepromazine and 0.72mg/kg BW)

414   followed by a pre-operative, subcutaneous injection of analgesic (ketoprofen, 5mg/kg BW). Post-

415   operative analgesic (subcutaneous injection of ketoprofen, 5mg/kg BW) was administered once

416   per day for 3 days following surgery. The surgical site was shaved and prepped with iodine and

417   ethanol swabs, and animals were placed in a stereotaxic apparatus for stereotaxic injections.

418   NMDA or viruses were delivered using a microinfusion pump (Harvard Apparatus, Cambridge,

419   MA, USA) connected to a 33-gauge microsyringe injector attached to a PE20 catheter and

420   Hamilton syringe. Flow rate was calibrated and set to 83.3nl/sec. Injectors were left in place for

421   2min post-injection to allow for complete delivery of the infusate. Specific viruses/drugs,

422   coordinates, and injection volumes for procedures are detailed below. Following the completion

423   of all injections, incision sites were closed using either surgical staples, or in the case of

424   subsequent placement of an indwelling cannula, simple interrupted sutures. Upon recovery from

425   anesthesia and return to dorsal recumbency, animals were returned to the home cage. All

426   behavioral procedures occurred 21 days after injections to allow for complete transduction and

427   expression of the viruses, or complete lesioning drugs. General intracranial injection procedures

428   were followed for all injection procedures below.

429

Chronic lesions of the HPCv

431   Lesion animals received bilateral excitotoxic HPCv lesions via intracranial injections of

432   N-methyl-d-aspartate (NMDA; 4ug in 200nL; 100uL per hemisphere) at the following

433   coordinates at three different sites along the rostrocaudal extent of the HPCv (59): [1] -4.8mm

434   AP, +/-5.0mm ML,   -7.5mm DV, [2] -5.5mm AP, +/-4.5mm ML, -7.0mm DV, and [3] -6.1mm

435   AP, +/-4.8mm ML, -7.0mm DV with control animals receiving vehicle saline in the same

436   location. The reference points for AP and ML coordinates were defined at bregma, and the

437   reference point for the DV coordinate was defined at the skull surface at the target site.

438   Bilateral HPCv lesion brains were histologically evaluated for the correct placement of

439   lesions in 1 out of 5 series of brain tissue sections. Neurons were visualized using

440   immunohistochemistry for the neuron specific antigen NeuN (see Immunohistochemistry). The

441   extent of NMDA lesions was determined postmortem by immunohistochemical detection of the

442   neuronal marker NeuN. Rats showing pronounced (~65%) loss of NeuN labeling within the

443   target region compared with the representative NeuN expression following sham injections in the

444   control group (average HPCv count of NeuN+ cells in control group) were included in data

445   analysis (34). Representative images in Fig. 1A.

446

447   **Acute and chronic disconnection of the CA1v to LS neural pathway**

448   Cre-dependent dual viral strategies were used to generate the following groups: [1] acute

449   chemogenetic disconnection of the CA1v to LS neural pathway (DREADDs; diagram of

450   approach in Fig. 2A), [2] chronic disconnection of the CA1v to LS neural pathway (caspase

451   lesion-induced; diagram of approach in Fig. 2B), and [3] a common/shared control group for

452   these two disconnection strategies. Regardless of group, all animals received a bilateral AAV

453   retro-cre injection in the LS (AAV2[retro]-hSYN1-EGFP-2A- iCre-WPRE; 200nL per side) at

454   the following stereotaxic coordinates (59): +0.84mm AP, +/-0.5mm ML, −4.8mm DV, all

455   defined at bregma.

456   According to experimental group, animals received a different virus delivered to the

457   CA1v subregion of the HPCv. All viruses were administered to the CA1v at the following

458   stereotaxic coordinates (59): −4.9mm AP defined at bregma, +/-4.8mm ML defined at bregma,

459   −7.8mm DV defined at skull surface at target site.

460   *[1] DREADDs group for reversible inactivation of CA1v to LS:* To allow reversible

461   chemogenetic inactivation of the CA1v to LS neural pathway, one group of animals received a

462   bilateral CA1v injection of a cre-dependent virus to drive expression of inhibitory designer

463   receptors activated by designer drugs (DREADDs), (AAV-Flex-hm4Di-tdTomato). This dual

16

464   viral strategy drives expression of inhibitory DREADDs exclusively in LS-projecting CA1v

465   neurons, which enables acute inactivation of these neurons by injection of the DREADDs ligand,

466   clozapine-N-oxide (CNO), at the time of behavioral testing.

467   *[2] Caspase group for chronic inactivation of CA1v to LS:* To allow chronic

468   disconnection of the CA1v to LS neural pathway, a second group of animals received a bilateral

469   CA1v cre-dependent caspase virus (AAV1-Flex-taCasp3-TEVp; 200nL per side) mixed with a

470   cre-dependent reporter virus (AAV-flex-tdTomato; 200nL per side) for histological verification.

471   This dual viral strategy drives expression of the apoptosis-mediator molecule caspase exclusively

472   in LS-projecting CA1v neurons, which induces apoptotic cell death in these neurons while

473   leaving other CA1v neurons intact.

474   *[3] Common control:* A common control group was generated so that the DREADDs and

475   caspase groups could both be compared to the same control group, instead of two different

476   control groups for the DREADDs and caspase groups, respectively. This allowed us to reduce

477   the number of animals needed for the same experimental objective. Thus, all animals received an

478   indwelling cannula and ICV injections of CNO as described below.

479   Immediately following viral injections, all animals were surgically implanted with a

480   unilateral indwelling intracerebroventricular (ICV) cannula (26-gauge, Plastics One, Roanoke,

481   VA) targeting the lateral ventricle (VL). Cannulae were implanted and affixed to the skull with

482   jeweler's screws and dental cement at the following stereotaxic coordinates: −0.9mm AP defined

483   at bregma, +1.8mm ML defined at bregma, −2.6mm DV defined at skull surface at site.

484   Placement for the VL cannula was verified by elevation of blood glucose resulting from an

485   injection of 210μg (2μL) of 5-thio-D-glucose (5TG) using an injector that extended 2mm beyond

486   the end of the guide cannula (60). A post-injection elevation of at least 100% of baseline

487   glycemia was required for subject inclusion. Animals that did not pass the 5TG test were retested

488   with an injector that extended 2.5mm beyond the end of the guide cannula and, upon passing the

489   5TG test, were subsequently injected using a 2.5mm injector instead of a 2mm injector for the

490   remainder of the study. Prior to behavioral testing where noted, all animals received an ICV

491   18mmol infusion (2uL total volume) of the DREADDs ligand clozapine N-oxide (CNO) (61),

492   rendering only DREADDs animals chemogenetically inactivated. CNO injections were hand

493   delivered using a 33-gauge microsyringe injector attached to a PE20 catheter and Hamilton

17

494   syringe through the indwelling guide cannulae. Injectors were left in place for 30sec to allow for

495   complete delivery of the CNO.

496   Cre-dependent DREADD expression targeting LS-projecting neurons in CA1v was

497   evaluated based on localization of the fluorescent reporter tdTomato. Immunohistochemistry for

498   red fluorescent protein (RFP) was conducted to amplify the tdTomato signal (see

499   Immunohistochemistry). Only animals with tdTomato expression restricted within CA1v neurons

500   were included in subsequent behavioral analyses. Representative images in Figs. 2C&D.

501   The general approach for neuronal apoptosis due to activation of cre-dependent caspase

502   targeting LS-projecting neurons in CA1v was validated in a separate cohort (n=8) based on

503   reduction of a cre-dependent fluorescent reporter tdTomato due to neuron cell death compared

504   with controls. The caspase group brains (which received a retro-cre virus in the LS in

505   conjunction with an injection of cre-dependent caspase virus mixed with a cre-dependent virus

506   that drives a tdTomato fluorescent reporter in the CA1v) were compared to control brains (that

507   received a retro-cre virus in the LS in conjunction with only a cre-dependent that drives a

508   tdTomato fluorescent reporter in the CA1v, which was equivalently diluted to match the caspase

509   injections). In both groups, immunohistochemistry for red fluorescent protein (RFP) was

510   conducted to amplify the tdTomato signal (see Immunohistochemistry). Confirmation of

511   successful caspase-driven lesions in the CA1v using this approach was evaluated by reduced

512   tdTomato fluorescence in comparison to control animals, with the expression of CA1v tdTomato

513   expression in the caspase group less than 15% of that observed in controls, on average

514   (Representative images in Supplementary Figs 2E&F). While this cohort allowed for successful

515   validation of the pathway-specific disconnection caspase approach, to improve the viability of

516   the animals for long-term behavioral analyses, the 3rd AAV with the fluorescent reporter (cre-

517   dependent tdTomato AAV) was omitted for cohorts undergoing behavioral analyses. For these

518   groups, histological confirmation for inclusion in subsequent statistical analyses was based on

519   identification of injections sites confined with the LS and CA1v, as observed using darkfield

520   microscopy.

521

522

523   **Identification of collateral targets of CA1v to LS projecting neurons**

524   Collateral targets of the CA1v to LS neural pathway were identified using a dual viral

525   approach (diagram of approach in Fig. 4A) where a retrograde vector was injected into the LS

526   (AAV2retro-hSyn1-eGFP-2A-iCre-WPRE; 200nL per side; coordinates as above), and a Cre-

527   dependent anterograde vector (AAV1-CAG-Flex-tdTomato-WPRE-bGH; 200nL per side;

528   coordinates as above) was injected in the CA1v. This latter injection drives tdTomato transgene

529   expression in CA1v neurons that project to the LS, which allows for brain-wide analyses of

530   collateral targets. After 3 weeks of incubation time to allow for complete transduction and

531   expression of the viruses, brains were collected, immunohistochemically processed, and imaged

532   as described below.

533

534   **Contralesional disconnection of the CA1v to mPFC neural pathway or the CA1v to LHA**

535   **neural pathway**

536   To functionally disconnect the CA1v to mPFC pathway (diagram of approach in Fig. 4E),

537   or the CA1v to LHA pathway (diagram of approach in Fig. 4J) lesion animals received a

538   unilateral excitotoxic CA1v lesion via an intracranial injection of NMDA (200nL) at the

539   following coordinates (36): −4.9mm AP defined at bregma, + or - 4.8mm ML defined at bregma

540   (left/right counterbalanced to be contralateral to mPFC or LHA lesion within-animal), −7.8mm

541   DV defined at skull surface at site, with control animals receiving vehicle saline injections in the

542   same location.

543   In addition to the CA1v lesion, CA1v to mPFC disconnect animals also received a

544   unilateral excitotoxic mPFC lesion via two intracranial injections of NMDA (4ug in 200nL;

545   100nL per injection) at the following coordinates (59): [1] +2.7mm AP, + or - 0.7mm ML

546   (left/right counterbalanced to be contralateral to CA1v lesion within-animal), −5.3mm DV and

547   [2] +3.0mm AP, + or - 0.7mm ML (left/right counterbalanced to be contralateral to CA1v lesion

548   within-animal), −4.7mm DV, with control animals receiving vehicle saline in the same location.

549   The reference points for all mPFC coordinates were defined at bregma.

550   In addition to the CA1v lesion, CA1v to LHA disconnect animals also received a

551   unilateral excitotoxic LHA lesion via an intracranial injection of NMDA (100nL per injection) at

552   the following coordinates (59): +2.9mm AP, + or – 1.1mm ML (counterbalanced to be

553   contralateral to CA1v lesion within-animal), −8.9mm DV, with control animals receiving vehicle

19

554   saline in the same location. The reference points for all LHA coordinates were defined at

555   bregma.

556   Contralesional brains were histologically evaluated for the correct placement of lesions by

557   visualizing neurons using immunohistochemistry for the neuron specific antigen NeuN (see

558   Immunohistochemistry). The extent of NMDA lesions was determined postmortem by

559   immunohistochemical detection of the neuronal marker NeuN. Rats showing pronounced (65%)

560   loss of NeuN labeling within the target region compared with a sham injection in the

561   contralateral side were included in data analysis (34).

562

563   **Identification of second order targets of CA1v to LS projecting neurons**

564   To identify second order targets of CA1v to LS-projecting neurons (diagram of approach

565   in Fig. 5A), animals received a bilateral injection of a transsynaptic Cre-inducing anterograde

566   vector into CA1v (AAV1-hSyn-Cre-WPRE-hGH; 200nL per side; coordinates as above) that

567   drives expression of Cre in both first-order (CA1v injection site) and 2nd-order (but not 3rd-

568   order) neurons via transsynaptic virion release (62, 63). This was combined with a bilateral

569   injection of a Cre-dependent anterograde vector in the LS (AAV1-CAG-Flex-tdTomato-WPRE-

570   bGH; 200nL per side, coordinates as above). This latter injection allows for anterograde tracing

571   from 1st-order LS targets receiving synaptic input from CA1v. After 3 weeks of incubation time

572   to allow for complete transduction and expression of the viruses, brains were collected,

573   immunohistochemically processed, and imaged as described below.

574   Data were entered using a custom built data-entry platform (Axiome C, created by JDH)

575   built around Microsoft Excel software and designed to facilitate entry of data points for all gray

576   matter regions across their atlas levels as described in a rat brain reference atlas: Brain Maps 4.0

577   (59). The Axiome C approach was used previously to facilitate the analysis of brain gene-

578   expression data (64). An ordinal scale, ranging from 0 (absent) to 7 (very strong), was used to

579   record the qualitative weight of anterograde labeling. An average value was then obtained for

580   each region across its atlas levels for which data were available. These data are summarized

581   graphically for a representative animal on a brain flatmap summary diagram (adapted from (65)).

582

583   **Food intake and body weight**

584   For the day prior to surgery (day 0) and for two weeks thereafter, 24h chow intake was

585   measured daily just prior to dark cycle onset to determine effects of experimental procedures on

586   food intake. Spillage was accounted for daily by collecting crumbs onto Techboard paper placed

587   under the cages of each animal. Additionally, animals were weighed daily just prior to dark cycle

588   onset to determine effects of experimental procedures on body weight.

589

590   **Meal pattern**

591   Meal size, meal frequency, meal duration, and cumulative 24h food intake were

592   measured using Biodaq automated food intake monitors (Research Diets, New Brunswick, NJ).

593   Rats (control n=7, caspase n=8, and DREADDs n=8) were acclimated to the Biodaq on ad

594   libitum chow for 3 days. Caspase group vs. control group feeding behavior data were collected

595   over a 5-day period (untreated, between-subjects design). The DREADDs group was tested using

596   a 2-treatment within-subjects design. Rats received 18mmol infusion of ICV CNO (2uL total

597   volume) or vehicle (daCSF, 33% dimethyl sulfoxide in artificial cerebrospinal fluid) 1h prior to

598   lights off and 24h feeding behavior was measured. Meal parameters were set at minimum meal

599   size=0.2g and maximum intermeal interval=600s.

600

601   **Appetitive food seeking spatial memory task**

602   To test visuospatial learning and memory for food reinforcement, we developed a novel

603   spatial food seeking task modified from the traditional Barnes maze procedure (6). Throughout

604   this paradigm, animals were maintained at 85% free-feeding body weight. The procedure

605   involves an elevated gray circular platform (diameter: 122cm, height: 140cm) consisting of 18

606   uniform holes (9.5cm diameter) spaced every twenty degrees around the outside edge. Under one

607   of the holes is a hidden tunnel (38.73cm L x 11.43cm W x 7.62cm D and a 5.08cm step).

608   Surrounding the table are distinct spatial cues on the wall (e.g. holiday lights, colorful shapes,

609   stuffed unicorn) that are readily visible to the animal. In contrast to the traditional Barnes Maze

610   where an animal uses the spatial cues to escape mildly aversive stimuli in the environment (e.g.

611   bright light and loud sound), this task utilizes food as motivation, such that each hidden tunnel

612   contained five 45mg sucrose pellets (Bio-Serv, Flemington, NJ). Additionally, a quiet white

613   noise (60dB) was used to drown out background noise and floor lamps were used for low-level

614   ambient lighting. On the first day, each animal underwent a habituation session consisting of

615   1min inside a transport bin under the table, 2min underneath the start box in the center of the

616   table, and 3min inside the hidden tunnel with 5 sucrose pellets. During training, each rat was

617   assigned a specific escape hole according to the position of the spatial cues with the location

618   counterbalanced across groups. Before each trial, animals were placed in the start box for 30

619   seconds. Animals were trained over the course of two 5-min trials per day for four days (five

620   days in contralesional experiments) to learn to use the spatial cues in order to locate the correct

621   hole with the hidden tunnel with sucrose pellets. After finding the correct hole and entering the

622   hidden tunnel during each 5min training session, animals were allowed to remain in the hidden

623   tunnel for 1 minute, and consistently consumed all 5 sucrose pellets at this time. In the event that

624   a rat did not find the correct hole during the 5min training session, the experimenter gently

625   guided the rat to the correct hole and were allowed to crawl in and then complete the training in

626   the same fashion as rats that found the hole on their own. Learning during training was scored

627   via animal head location tracking by AnyMaze Behavior Tracking Software (Stoelting Co.,

628   Wood Dale, IL). The incorrect hole investigations prior to finding the correct hole with sucrose

629   pellets ("errors before correct hole") as well as time to finding the correct hole ("latency to

630   correct hole") were calculated as an average of the two trials per day, and examined across days

631   of training.

632   After the conclusion of training, rats had a two-day break where no procedures occurred,

633   then were tested in a single 2min memory probe in which the hidden tunnel and sucrose pellets

634   were been removed. All animals received an ICV 18mmol infusion of CNO (2uL total volume)

635   1h prior to the memory probe, rendering only DREADDs animals chemogenetically inactivated

636   by CNO. In the memory probe, the ratio of the correct hole plus adjacent hole investigations over

637   the total number of hole investigations were calculated via animal head location tracking by

638   AnyMaze Behavior Tracking Software (Stoelting, Wood Dale, IL). This dependent variable was

639   selected a priori instead of correct hole only investigations based on recent findings

640   demonstrating that taste-responsive hippocampal neurons exhibit weaker spatial selectivity in

641   comparison to non-taste-responsive hippocampal neurons (66). When establishing and refining

642   the food-reinforced spatial memory procedure in multiple cohorts of rats, our preliminary data

643   revealed that memory probe effects in normal/control animals are either stronger in the 1st

644   minute, or in the 1st two minutes combined (but not the 2nd minute alone), with some cohorts

645   showing larger paradigm effects in minute 1, and others in minutes 1+2. Thus, for all

22

646   experiments presented we analyzed both the 1st minute and the 1st two minutes combined based

647   on an a priori determination from our preliminary studies. A diagram of the apparatus used for

648   the spatial foraging task is included in Fig. 1B.

649   During training sucrose pellets were taped underneath all of the holes to preclude

650   olfactory-based search strategies during training. Importantly, the memory probe test does not

651   include any sucrose pellets in the apparatus at all, and therefore there is no possibility of sucrose

652   odor cues to influence memory probe performance.

653

654   **Appetitive water seeking spatial memory task**

655   We modified our spatial food seeking task to utilize water reward instead of food reward.

656   Throughout this paradigm, animals were water restricted and received 90-min access to water

657   daily (given at least 1hr after the termination of behavioral procedures each day). In addition to

658   the habituation parameters described above, animals in this task were subjected to two 10-min

659   habituation sessions in the hidden tunnel with a full water dish prior to training, which allowed

660   them to become accustomed to reliably drinking from the water dish in the hidden tunnel.

661   Training procedures were the same as for the food-based task above, except instead of sucrose

662   pellets in the hidden tunnel, a water dish containing ~100 mL of water was placed in the back of

663   the hidden tunnel during training, and animals were allowed to remain in the hidden tunnel for

664   2min (instead of 1min, as above). Each animal consumed a minimum of 2mL of water during

665   this time for the training sessions. This newly-developed procedure allowed us to test spatial

666   learning and memory motivated by water reward using similar apparatus and stimulus conditions

667   to the food-reinforced task.

668

669   **Aversive spatial memory escape task (Barnes maze)**

670   To test visuospatial learning and memory for escape reinforcement, we used a modified

671   traditional Barnes maze procedure, which is a visuospatial-based escape task (6). Procedures

672   were exactly the same as above (appetitive spatial memory food seeking and water seeking tasks,

673   using the same apparatus, in the same room, and with the same visuospatial cues) aside from the

674   omission of the sucrose pellets or water dish in the hidden tunnel, the presence of mildly aversive

675   bright (120W) overhead lighting instead of dim ambient lighting, and a mildly aversive loud

676   white noise (75dB) instead of a quiet white noise (60dB). This allowed us to test spatial learning

23

677 and memory motivated by escape from aversive stimuli in a nearly-identical procedure to our

678 spatial foraging test for learning and memory motivated by palatable food or water consumption.

679 A diagram of the apparatus used for the spatial escape task is included in Fig. 1B.

680

681 **Social transmission of food preference (STFP)**

682 To examine food-related memory based on social- and olfactory-based cues, we utilized

683 the social transmission of food preference (STFP) task and adapted protocols from (32, 42, 67,

684 68). Briefly, untreated normal adult rats are designated as 'Demonstrators', while experimental

685 groups are designated as 'Observers'. Demonstrators and Observers are habituated to a powdered

686 rodent chow [LabDiet 5001 (ground pellets), LabDiet, St. Louis, MO] overnight. 24h later,

687 Observers are individually paired with demonstrators and habituated to social interaction, where

688 rat pairs are placed in a social interaction arena (23.5cm W × 44.45cm L × 27cm H clear plastic

689 bin with Sani-chip bedding) and allowed to interact for 30min. Both Observers and

690 Demonstrators are returned to their home cages and food is withheld for 23hr prior to the social

691 interaction. For the social interaction, Demonstrators are given the opportunity to consume one

692 of two flavors of powdered chow (flavored with 2% marjoram or 0.5% thyme; counterbalanced

693 according to group assignments) for 30min in a room separate from Observers. Our pilot studies

694 and previous published work (68, 69) show that rats equally prefer these flavors of chow. The

695 Demonstrator rat is then placed in the social interaction arena with the Observer rat, and the pairs

696 are allowed to socially interact for 30min. Observers are then returned to their home cage and

697 allowed to eat *ad libitum* for 1h and then food is removed. The following day, the 23h food-

698 deprived Observer animals are given a home cage food preference test for either the flavor of

699 chow paired with the Demonstrator animal, or a novel, unpaired flavor of chow that is a flavor

700 that was not given to the Demonstrator animal (2% marjoram vs. 0.5% thyme; counterbalanced

701 according to group assignments). All animals received an ICV 18mmol infusion of CNO (2uL

702 total volume) 1h prior to the social interaction session, rendering only DREADDs animals

703 chemogenetically inactivated by CNO. Food intake (1h) was recorded with spillage accounted

704 for by collecting crumbs onto Techboard paper that is placed under the cages of each animal.

705 The % preference for the paired flavor is calculated as: 100*Demonstrator-paired flavored chow

706 intake/Demonstrator + Novel flavored chow intake. In this procedure, normal untreated animals

707   learn to prefer the Demonstrator paired flavor based on social interaction and smelling the breath

708   of the Demonstrator rat (32, 42, 67-69). A diagram of the STFP procedure is included in Fig. 3E.

709

710   **Zero maze**

711   The zero maze behavioral paradigm was used to evaluate anxiety-like behavior. The zero

712   maze apparatus used was an elevated circular track, divided into four equal length sections. Two

713   zones were open with 3 cm high curbs ('open zones'), whereas the two other zones were closed

714   with 17.5 cm high walls ('closed zones'). All animals received an ICV 18mmol infusion of CNO

715   (2uL total volume) 1h prior to testing, rendering only DREADDs animals chemogenetically

716   inactivated by CNO. Behavioral testing was performed during the light cycle. Animals were

717   placed in the maze for a single, 5min trial in which the location of the center of the animal's

718   body was measured by AnyMaze Behavior Tracking Software (Stoelting, Wood Dale, IL). The

719   apparatus was cleaned with 10% ethanol in between animals. During the trial, the number of

720   open zone entries and total time spent in open sections (defined as body center in open sections)

721   were measured, which are each indicators of anxiety-like behavior in this procedure. A diagram

722   of the zero maze apparatus is included in Fig. 3G.

723

724   **Open field**

725   An open field test was used to evaluate general levels of locomotor activity. The

726   apparatus used for the open field test was an opaque gray plastic bin (60cm × 56cm), which was

727   positioned on a flat table in an isolated room with a camera directly above the center of the

728   apparatus. Desk lamps were positioned to provide indirect lighting to all corners of the maze

729   such that the lighting in the box uniformly measured 30 lux throughout. All animals received an

730   ICV 18mmol infusion of CNO (2uL total volume) 1h prior to testing rendering only DREADDs

731   animals chemogenetically inactivated by CNO. Behavioral testing began at dark onset. At the

732   start of the 10min test, each animal was placed in the open field apparatus in the same corner

733   facing the center of the maze. The location of the center of the animal's body was measured with

734   the AnyMaze Behavior Tracking Software (Stoelting, Wood Dale, IL). Total distance traveled

735   was measured by tracking movement from the center of the animal's body throughout the test.

736

737   **Immunohistochemistry**

25

738   Rats were anesthetized via an intramuscular injection of an anesthesia cocktail (ketamine

739   90mg/kg BW xylazine, 2.8mg/kg BW and acepromazine and 0.72mg/kg BW) then transcardially

740   perfused with 0.9% sterile saline (pH 7.4) followed by 4% paraformaldehyde (PFA) in 0.1M

741   borate buffer (pH 9.5; PFA). Brains were dissected from the skull and post-fixed in PFA with

742   15% sucrose for 24h, then flash frozen in isopentane cooled in dry ice. Brains were sectioned to

743   30μm thickness on a freezing microtome. Sections were collected in 5-series and stored in

744   antifreeze solution at −20°C until further processing. General fluorescence IHC labeling

745   procedures were performed as follows. The antibodies and dilutions that were used are as

746   follows: [1] For lesion histology using the neuron-specific protein NeuN, the rabbit anti-NeuN

747   primary antibody (1:1000, Abcam) was used followed by a donkey anti-rabbit conjugated to

748   AF488 (1:500, Jackson Immunoresearch). [2] To amplify the native tdTomato signal for

749   neuroanatomical tracing or DREADDs histology, the rabbit anti-RFP primary antibody (1:2000,

750   Rockland) was used followed by a donkey anti-rabbit conjugated to Cy3 (1:500, Jackson

751   Immunoresearch). [3] To amplify the native GFP signal for LS injection site histology, the

752   chicken anti-GFP primary antibody (1:500, Abcam) was used followed by a donkey anti-chicken

753   secondary antibody conjugated to AF488 (1:500, Jackson Immunoresearch). Antibodies were

754   prepared in 0.02M potassium phosphate buffered saline (KPBS) solution containing 0.2% bovine

755   serum albumin and 0.3% Triton X-100 at 4°C overnight. After thorough washing with 0.02M

756   KPBS, sections were incubated in secondary antibody solution. All secondary antibodies were

757   obtained from Jackson Immunoresearch and used at 1:500 dilution at 4°C, with overnight

758   incubations (Jackson Immunoresearch; West Grove, PA, USA). Sections were mounted and

759   coverslipped using 50% glycerol in 0.02 M KPBS and the edges were sealed with clear nail

760   polish. Photomicrographs were acquired using a Nikon 80i (Nikon DSQI1,1280X1024

761   resolution, 1.45 megapixel) under epifluorescence or darkfield illumination.

762   Lesions and virus expression were quantified in one out of five series of brain tissue sections and

763   analyses were performed in sections from Swanson Brain Atlas level 34-36 (59). The inclusion /

764   exclusion criteria are described above in the methods of each of these experiments.

765

766   **Statistics**

767   Data are expressed as mean +/- SEM. Differences were considered to be statistically

768   significant at $p<0.05$. All variables were analyzed using the advanced analytics software package

769   Statistica (StatSoft, Tulsa, OK, USA). For all measures of food intake, body weight, and

770   errors/latency during spatial foraging and spatial escape task training, differences between

771   groups were evaluated using two-way repeated measures ANOVAs (treatment x time). For

772   lesion experiments, measures during spatial foraging and spatial escape task probes, differences

773   between groups were evaluated using two-tailed independent two-sample Student's t-tests. For

774   CA1v to LS disconnection experiments, measures during spatial foraging and spatial escape task

775   probes, the STFP paradigm, the zero maze paradigm, and the open field test, differences between

776   groups were evaluated using one-way ANOVAs. Significant ANOVAs were analyzed with a

777   Fisher's LSD posthoc test where appropriate. Outliers were identified as being more extreme

778   than the median +/- 1.5 * interquartile range. For all experiments, assumptions of normality,

779   homogeneity of variance (HOV), and independence were met where required.

780

781

782   **CONFLICT OF INTEREST**

783   No conflicts of interest.

784

785   **ACKNOWLEDGEMENTS**

790

791

Figure 1

A — NeuN (lesion) / NeuN (sham); CA3v, CA1v, DG, alv

B — (behavioral arena schematic)

C

D

E — Spatial foraging training (errors)

F — Spatial foraging training (latency)
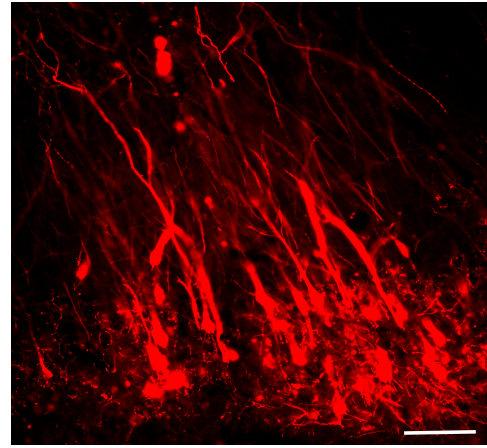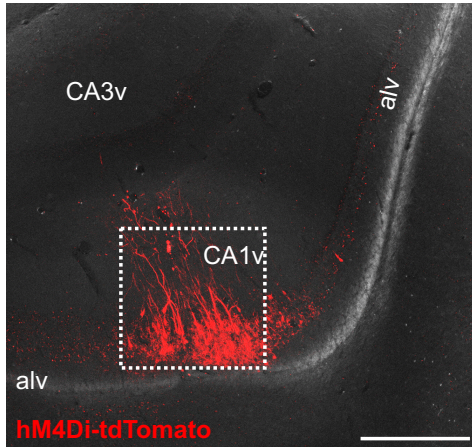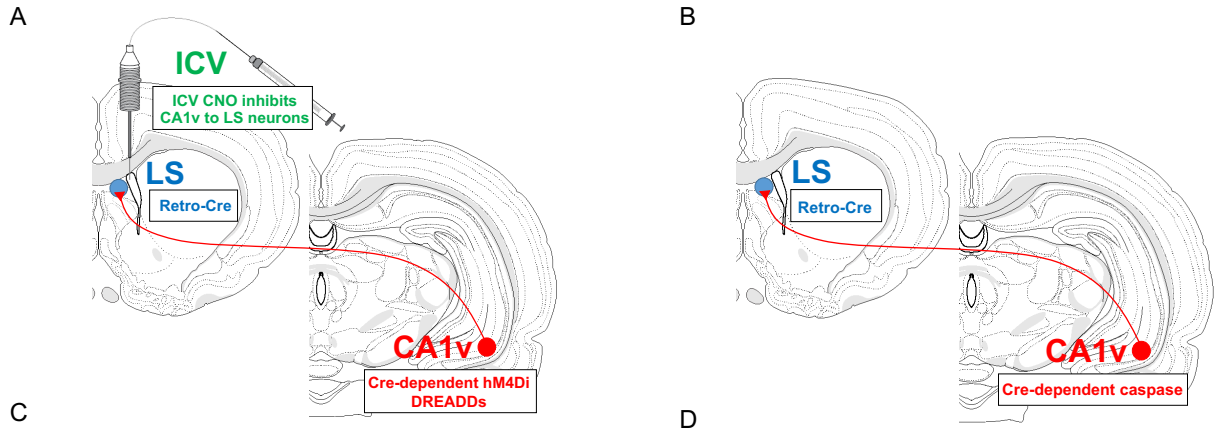
G — Memory probe
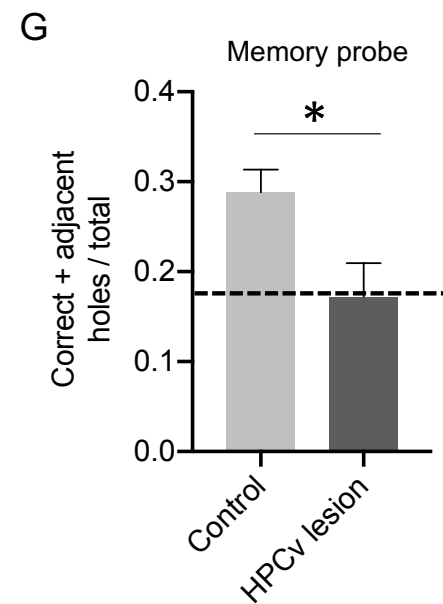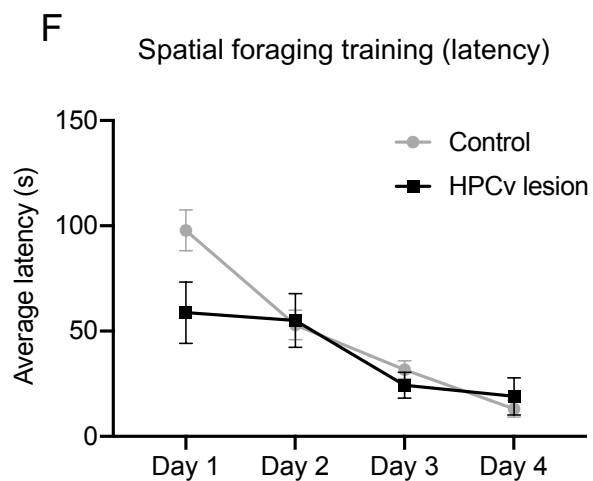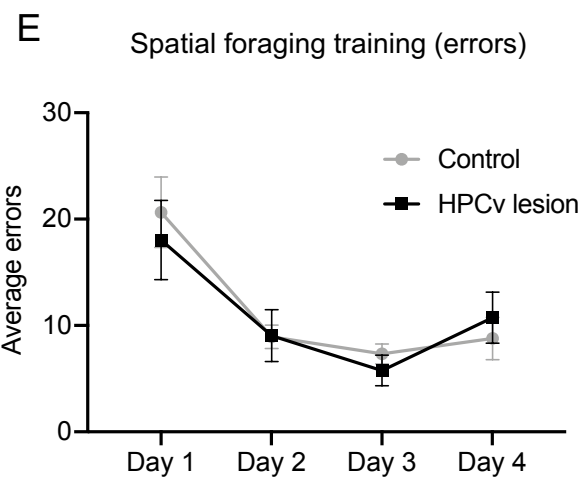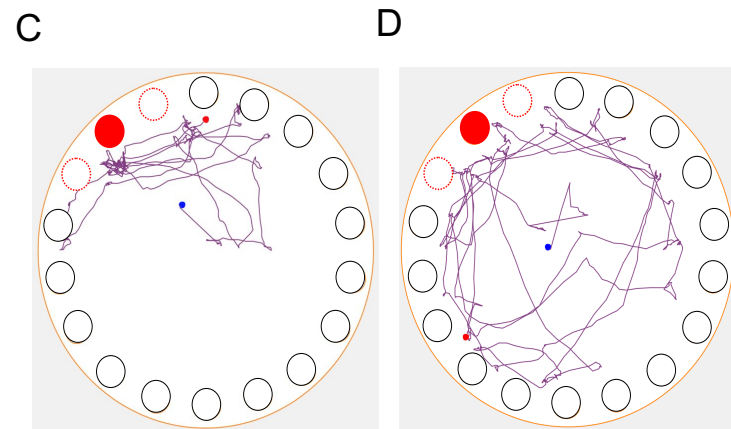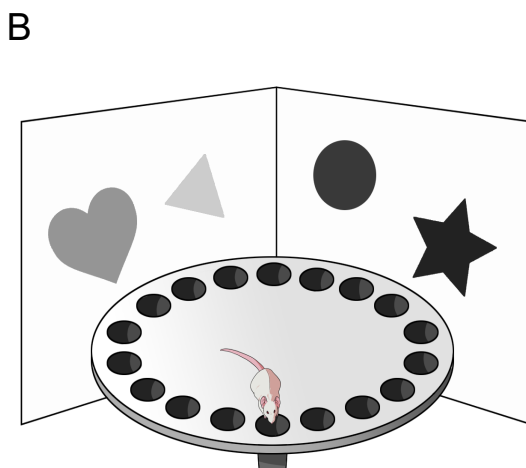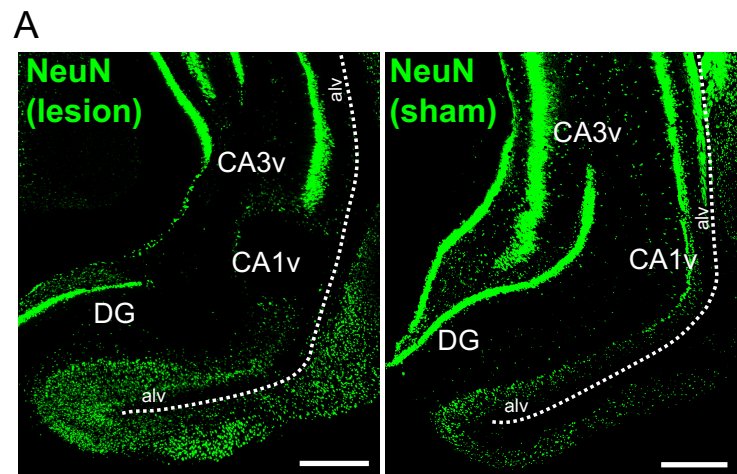
792 **Figure 1. Bilateral HPCv lesions impair spatial memory for food location.** Representative

793 HPCv lesion histology with NeuN immunohistochemistry (A; scale bars 500μm). Spatial

794 foraging task apparatus (B). Representative navigation paths of a control animal preferentially

795 investigating correct (filled red) and adjacent holes (outlined orange) during spatial foraging

796 memory probe (C). Representative navigation path of HPCv lesioned animal during spatial

797 foraging memory probe (D). Bilateral HPCv lesions did not impair learning of the spatial

798 foraging task compared to controls, as measured by errors before locating correct hole during

799 task training (E) and latency to locate correct hole during task training (F). Bilateral HPCv

800 lesions impaired retention of the spatial foraging task, as measured by the ratio of investigation

801 of correct plus adjacent holes over total investigated during the first minute of the task ($p<0.05$;

802 G). There were no group differences observed when evaluated over the entire two minutes of the

803 task (H). Dotted line indicates chance performance level (0.167). For graphs 1D-G, lesion n = 11,
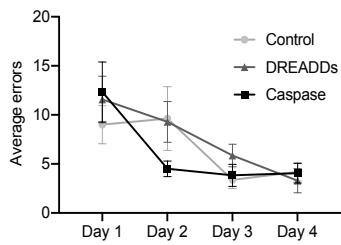
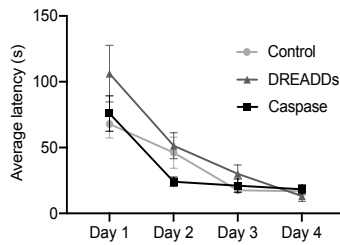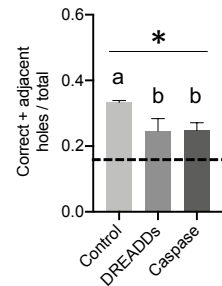804 control n = 18. All values expressed as mean +/- SEM.

805

806

Figure 2

A ICV
ICV CNO inhibits CA1v to LS neurons
LS
Retro-Cre
CA1v
Cre-dependent hM4Di DREADDs

B
LS
Retro-Cre
CA1v
Cre-dependent caspase

C CA3v   alv
CA1v
alv
hM4Di-tdTomato

D

E Spatial food seeking training (errors)
Average errors
Control
DREADDs
Caspase
Day 1 Day 2 Day 3 Day 4

F Spatial food seeking training (latency)
Average latency (s)
Control
DREADDs
Caspase
Day 1 Day 2 Day 3 Day 4

G Memory probe
Correct + adjacent holes / total
*
a   b   b
Control DREADDs Caspase

H Spatial water seeking training (errors)
Average errors
Control
DREADDs
Caspase
Day 1 Day 2 Day 3 Day 4

I Spatial water seeking training (latency)
Average latency (s)
Control
DREADDs
Caspase
Day 1 Day 2 Day 3 Day 4

J Memory probe
Correct + adjacent holes / total
*
a   b   b
Control DREADDs Caspase

K Spatial escape training (errors)
Average errors
Control
DREADDs
Caspase
Day 1 Day 2 Day 3 Day 4
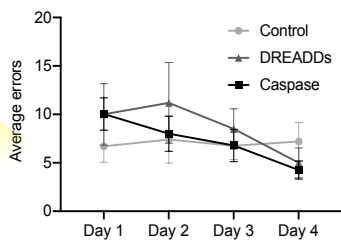
L Spatial escape training (latency)
Average latency (s)
Control
DREADDs
Caspase
Day 1 Day 2 Day 3 Day 4
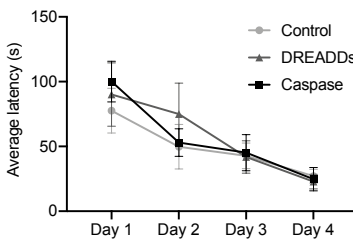
M Memory probe
Correct + adjacent holes / total
Control DREADD Caspase
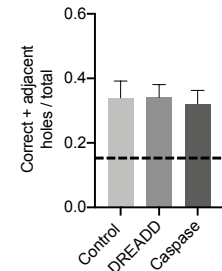
807 **Figure 2. Reversible and chronic CA1v to LS neural disconnection impairs spatial memory**

808 **for food and water location but not for escape location.** Diagram of dual viral approach using

809 a cre-dependent inhibitory DREADDs approach to reversibly disconnect CA1v to LS neural

810 pathway (A). Diagram of dual viral approach using a cre-dependent caspase approach to

811 chronically disconnect CA1v to LS neural pathway (B). Representative injection site in CA1v

812 demonstrating LS-projecting neurons infected with inhibitory DREADDs, which simultaneously

813 drives expression of a fluorescent tdTomato transgene (C, D; scale bars 500μm and 100μm,

814 respectively). Neither reversible (DREADDs) nor chronic (caspase) disconnection of the CA1v

815 to LS pathway impaired learning of the spatial food seeking task compared to controls, as

816 measured by errors before correct hole during task training (E) and latency to correct hole during

817 task training (F). Both reversible and chronic disconnection of the CA1v to LS pathway impaired

818 retention of the food location as measured by the ratio of investigation of correct plus adjacent

819 holes over total investigations during entire two minutes of the task ($p < 0.05$; G). Likewise,

820 reversible (DREADDs) and chronic (caspase) disconnection of the CA1v to LS pathway did not

821 impair learning of the spatial water seeking task compared to controls, as measured by errors

822 before correct hole during task training (H) and latency to correct hole during task training (I),

823 but impaired memory retention of the water location during the probe (J). In contrast,

824 disconnection of the CA1v to LS pathway either reversibly (DREADDs) or chronically (caspase)

825 did not impair performance on the spatial escape task. There were no differences in learning as

826 measured by errors before correct hole during task training (K) and latency to correct hole during

827 task training (L). Unlike the spatial foraging task, retention of the spatial escape task was not

828 impaired by reversible nor chronic disconnection of the CA1v to LS pathway (M). For graphs

829 2E-G (CA1v to LS disconnect cohort 1), DREADDs n=6, caspase n=10, control n=8. For graphs

830 2H-J (CA1v to LS disconnect cohort 3), DREADDs n=8, caspase n=8, control n=7). For graphs

831 2K-M (CA1v to LS disconnect cohort 2), DREADDs n=8, caspase n=12, control n=10. Dotted

832 line indicates chance performance level (0.167). All values expressed as mean +/- SEM.

833

834

Figure 3

A

Day 1

Demonstrators and observers habituate to social interaction
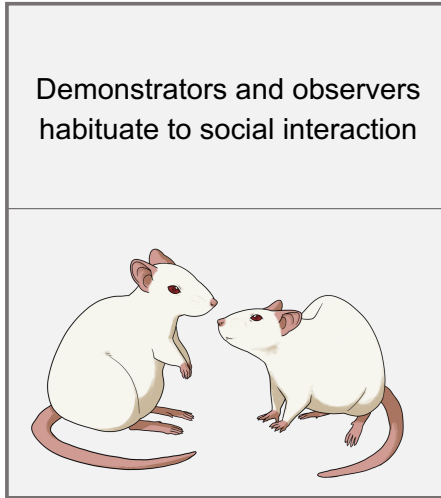
Day 2

Demonstrators consume flavored chow (chow A) prior to social interaction

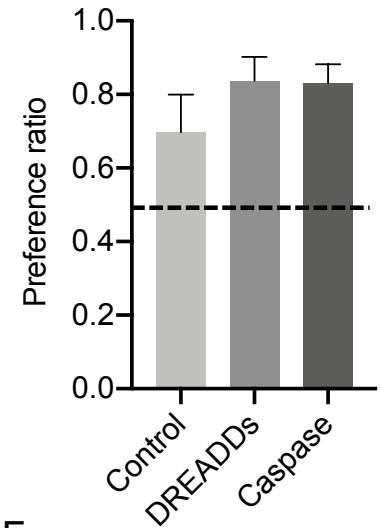Demonstrators and observers have a 30min social interaction

Day 3

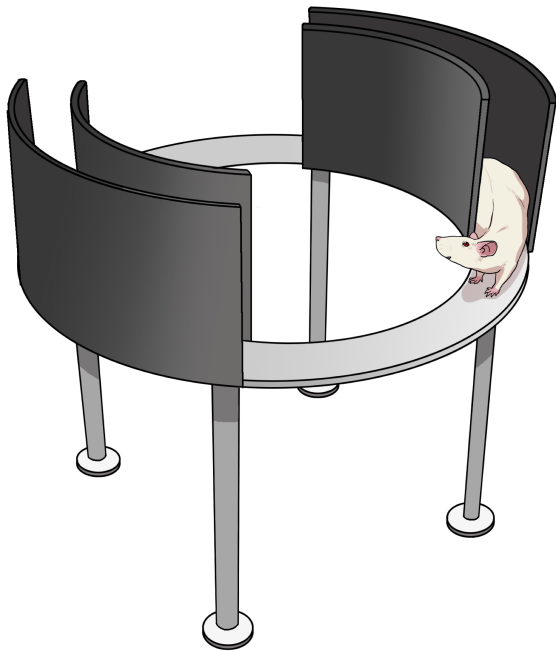Food-restricted observers are given a 60min flavor preference test (chow A vs. novel chow B)

B

Social transmission of food preference

Preference ratio

Control   DREADDs   Caspase

C

D

Zero maze: Open zone time

Time in open zones (s)

Control   DREADDs   Caspase
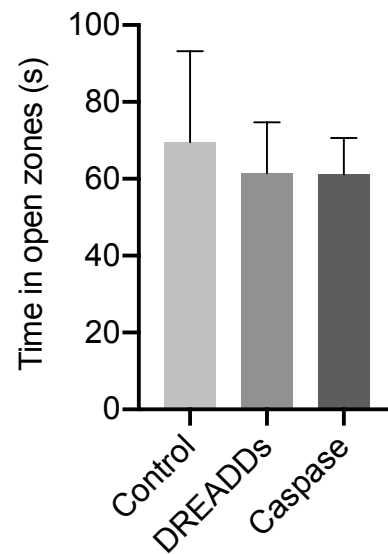
E

Zero maze: Open zone entries

Entries to open zones

Control   DREADDs   Caspase

F

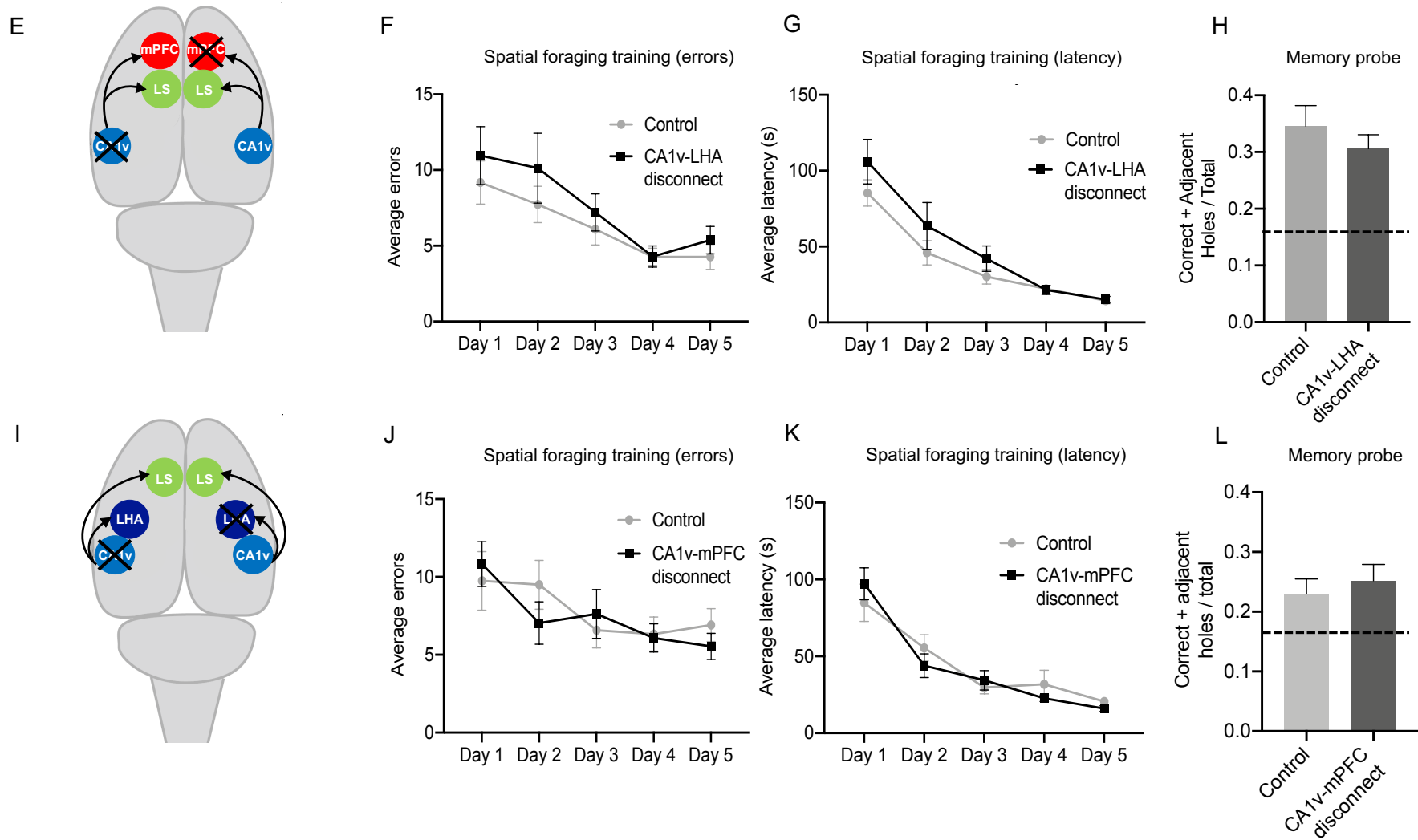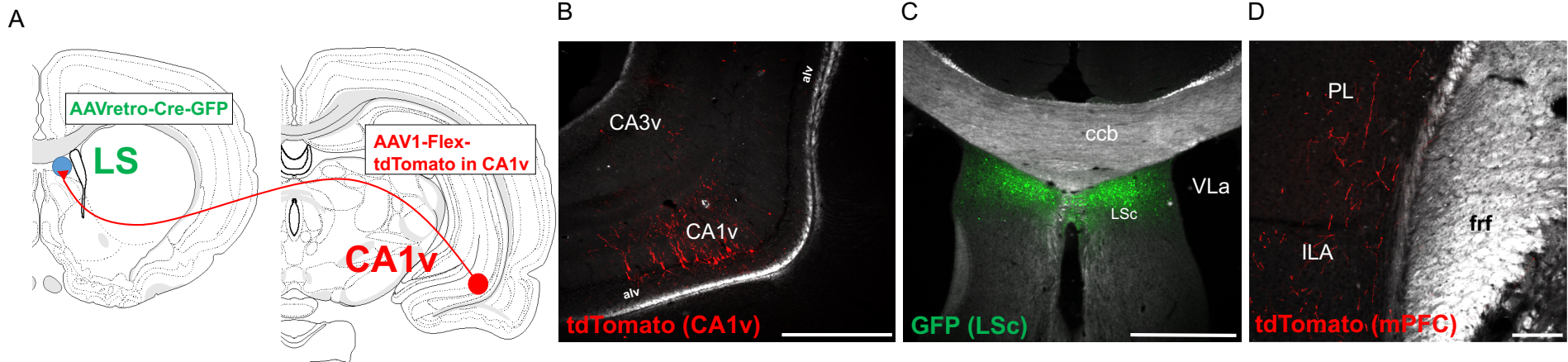Open field

Distance traveled (m)
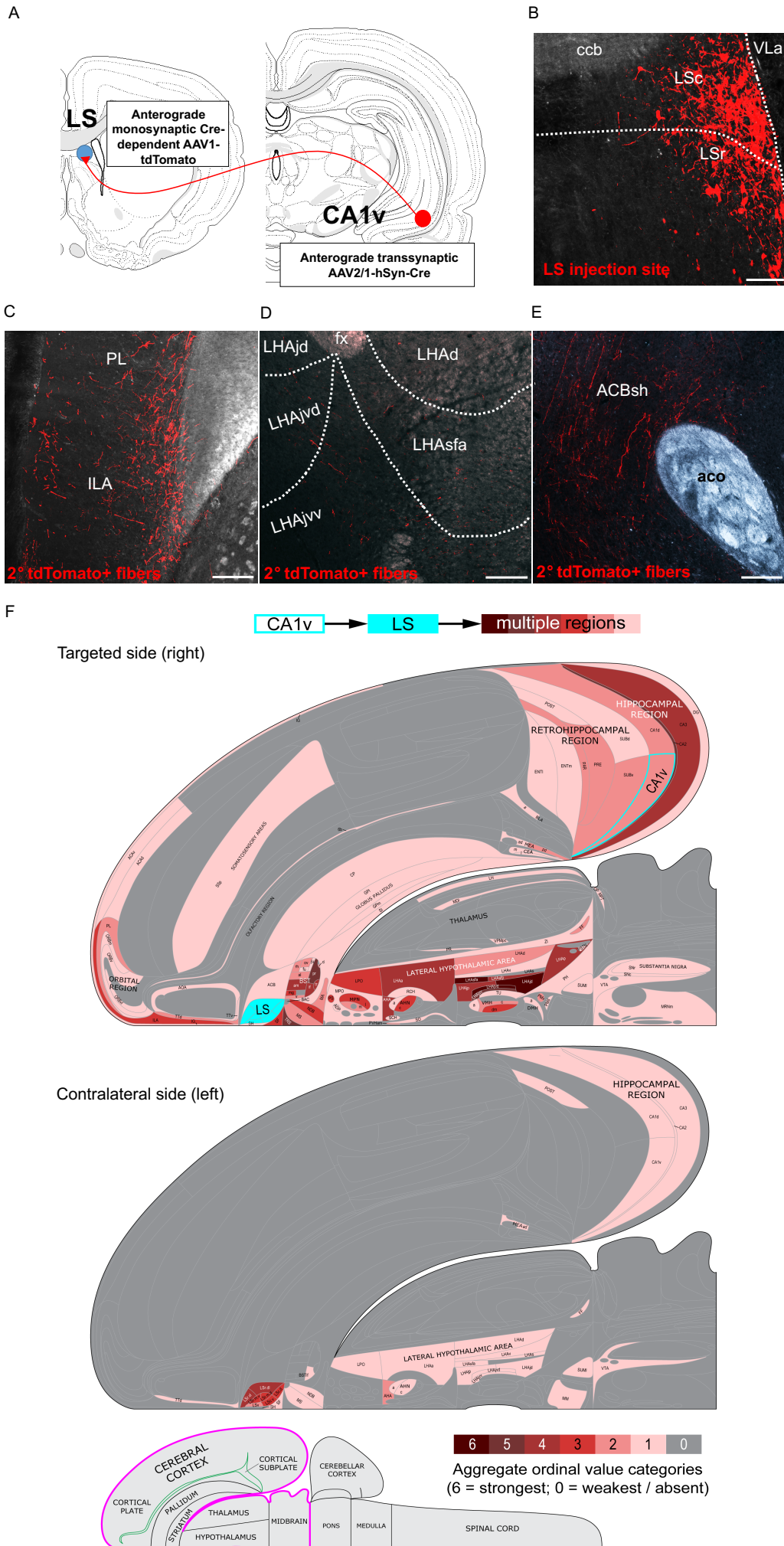
Control   DREADDs   Caspase
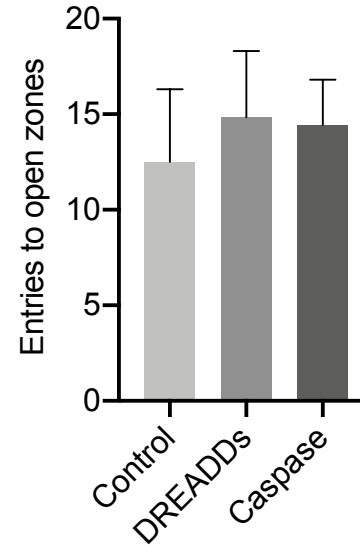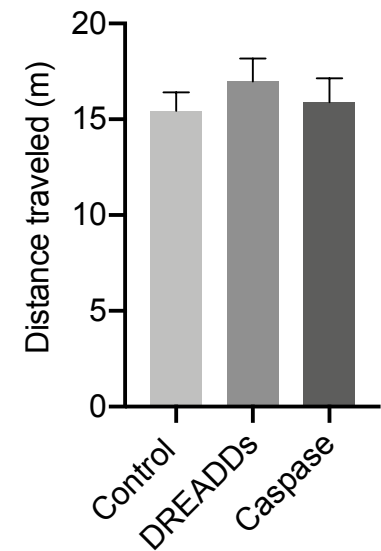
835   **Figure 3. Neither reversible nor chronic CA1v to LS neural disconnection impair spatial**

836   **memory for escape location, social transmission of food preference, anxiety-like behavior,**

837   **or general locomotor activity levels.** Diagram of the social transmission of food preference

838   (STFP) task (A). Neither reversible nor chronic disconnection of the CA1v to LS pathway impair

839   STFP learning compared to controls, as measured by a food preference ratio (B), with the dotted

840   line indicating chance preference level (0.50). Diagram of the zero maze apparatus (C). Anxiety-

841   like behavior was not influenced by reversible or chronic disconnection of the CA1v to LS

842   pathway compared to controls, as measured by performance in the zero maze task, specifically

843   time in open zones (D) and entries into open zones (E). Neither chronic nor reversible CA1v to

844   LS disconnection affected open field performance compared to controls, as measured by total

845   distance traveled (F). For graphs 3B, 3D, and 3E (CA1v to LS disconnect cohort 1), DREADDs

846   n=6, caspase n=10, control n=8. For graph 3F (CA1v to LS disconnect cohort 2), DREADDs

847   n=8, caspase n=12, control n=10. All values expressed as mean +/- SEM.

848

849

Figure 4

A AAVretro-Cre-GFP
LS
AAV1-Flex-tdTomato in CA1v
CA1v

B CA3v
alv
CA1v
alv
tdTomato (CA1v)

C ccb
VLa
LSc
GFP (LSc)

D PL
ILA
frf
tdTomato (mPFC)

E

F Spatial foraging training (errors)
Average errors
Day 1 Day 2 Day 3 Day 4 Day 5
Control
CA1v-LHA disconnect

G Spatial foraging training (latency)
Average latency (s)
Day 1 Day 2 Day 3 Day 4 Day 5
Control
CA1v-LHA disconnect

H Memory probe
Correct + Adjacent Holes / Total
Control
CA1v-LHA disconnect

I

J Spatial foraging training (errors)
Average errors
Day 1 Day 2 Day 3 Day 4 Day 5
Control
CA1v-mPFC disconnect

K Spatial foraging training (latency)
Average latency (s)
Day 1 Day 2 Day 3 Day 4 Day 5
Control
CA1v-mPFC disconnect

L Memory probe
Correct + adjacent holes / total
Control
CA1v-mPFC disconnect

850 **Figure 4. Neither CA1v to mPFC nor CA1v to LHA disconnection impairs spatial memory**

851 **for food location.** Diagram of dual viral approach to identify collateral targets of the CA1v to

852 LS neural pathway (A). Representative CA1v injection site from collateral identification

853 approach (B; scale bar 500μm). Representative LS injection site from collateral identification

854 approach (C; scale bar 500μm). Representative image collateral axons of the CA1v to LS

855 pathway located in the mPFC (D; scale bar 50μm). Diagram of contralesional approach to

856 functionally disconnect the CA1v to mPFC neural pathway (E). Disconnection of the CA1v to

857 mPFC neural pathway did not influence learning of the spatial foraging task compared to

858 controls, as measured by errors before correct hole during training (F) and latency to correct hole

859 during training (G). Disconnection of the CA1v to mPFC pathway did not influence retention of

860 the spatial foraging task in the memory probe (H). Diagram of contralesional approach to

861 functionally disconnect the CA1v to LHA neural pathway (I). Disconnection of the CA1v to

862 LHA neural pathway did not influence learning of the spatial foraging task compared to controls,

863 as measured by errors before correct hole during training (J) and latency to correct hole during

864 training (K). Disconnection of the CA1v to LHA pathway did not influence retention of the

865 spatial foraging task in the memory probe (L). For graphs 4F-I, CA1v to mPFC disconnect n=12,

866 control n=12. For graphs 4K-N, CA1v to LHA disconnect n=12, control n=11. All values

867 expressed as mean +/- SEM.

868

869

Figure 5

A

LS

Anterograde monosynaptic Cre-dependent AAV1-tdTomato

CA1v

Anterograde transsynaptic AAV2/1-hSyn-Cre

B

ccb

VLa

LSc

LSr

LS injection site

C

PL

ILA

2° tdTomato+ fibers

D

LHAjd

fx

LHAd

LHAjvd

LHAsfa

LHAjvv

2° tdTomato+ fibers

E

ACBsh

aco

2° tdTomato+ fibers

F

CA1v → LS → multiple regions

Targeted side (right)

HIPPOCAMPAL REGION

RETROHIPPOCAMPAL REGION

CA1v

THALAMUS

LATERAL HYPOTHALAMIC AREA

SUBSTANTIA NIGRA

ORBITAL REGION

GLOBUS PALLIDUS

SOMATOSENSORY AREAS

OLFACTORY REGION

LS

Contralateral side (left)

HIPPOCAMPAL REGION

LATERAL HYPOTHALAMIC AREA

| 6 | 5 | 4 | 3 | 2 | 1 | 0 |

Aggregate ordinal value categories
(6 = strongest; 0 = weakest / absent)

CEREBRAL CORTEX

CORTICAL SUBPLATE

CEREBELLAR CORTEX

CORTICAL PLATE

PALLIDUM

STRIATUM

THALAMUS

HYPOTHALAMUS

MIDBRAIN

PONS

MEDULLA

SPINAL CORD

870   **Figure 5. Identification of second-order neural projections downstream of CA1v to LS**

871   **projections.** Diagram of dual viral approach to identify brain regions that are second-order (2°)

872   targets of the CA1v to LS neural pathway (A). Representative LS injection site from second

873   order identification approach (B; scale bar 100μm). Representative image of second-order fibers

874   of the CA1v to LS pathway within the mPFC (C; scale bar 200μm). Representative image of

875   second-order fibers of the CA1v to LS pathway within the LHA (D; scale bar 200μm).

876   Representative image of second-order fibers of the CA1v to LS pathway within the ACB (E;

877   scale bar 200μm). Summary of the projection targets of LS neurons that receive input from

878   CA1v (F). The outputs of the right side of LS neurons receiving CA1v input are represented at

879   the macroscale (gray matter region resolution) on a partial flatmap representation of the rat

880   forebrain, adapted from (65). Connection weights are represented block colors for each region

881   following an ordinal scale ranging from weakest (0 = very weak or absent) to strongest (6 =

882   strong), as there were no 7 (very strong) values. The inset at lower left represents one side of the

883   brain with the part represented in the upper diagrams outlined in magenta.
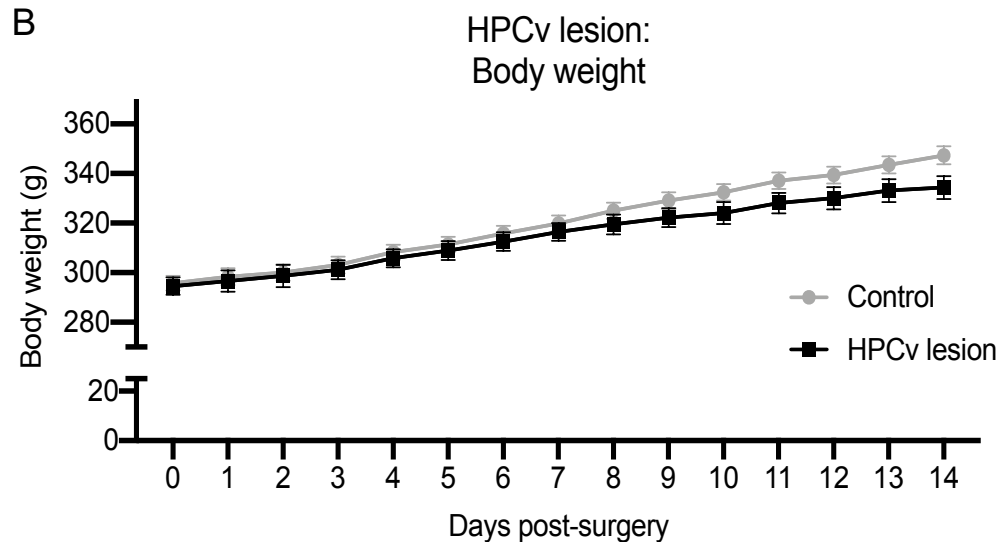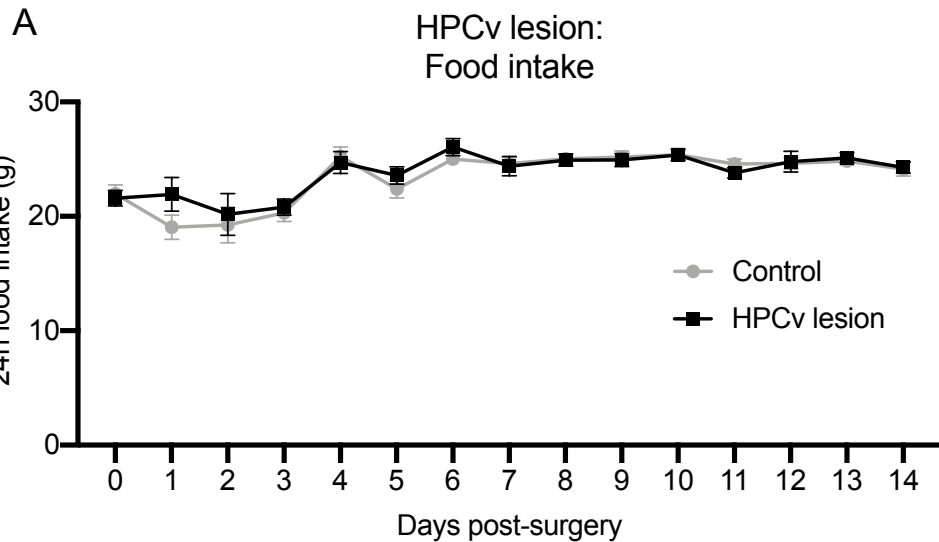
884

885

886 **SUPPLEMENTARY INFORMATION**
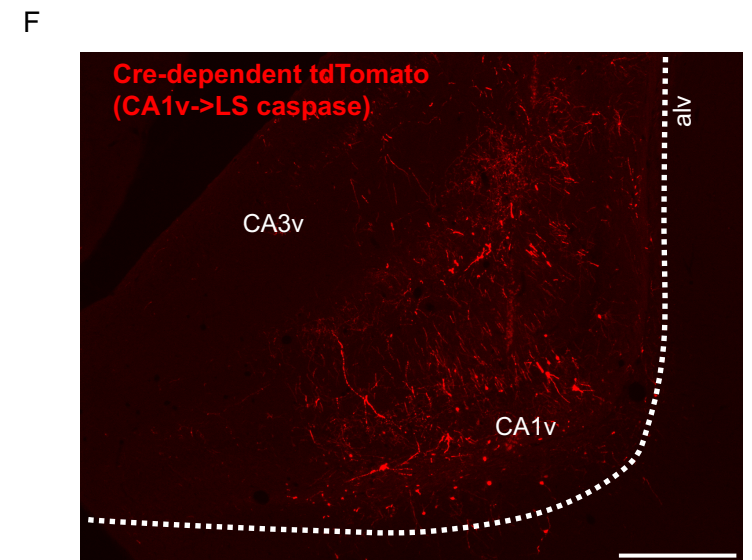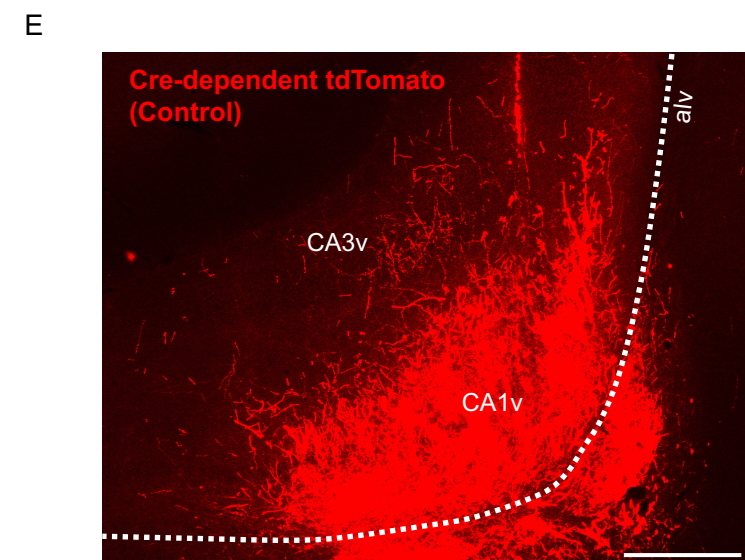
887

888

Supplemental Figure 1

A

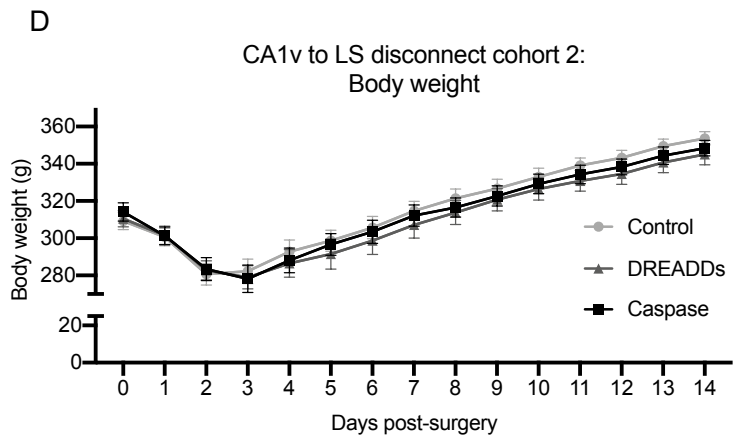HPCv lesion:
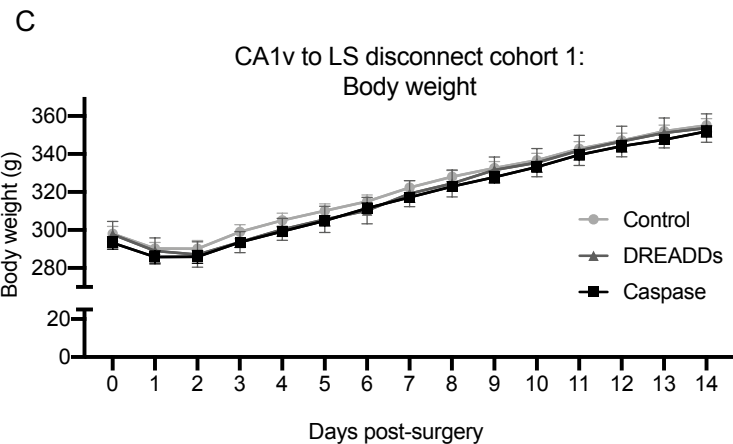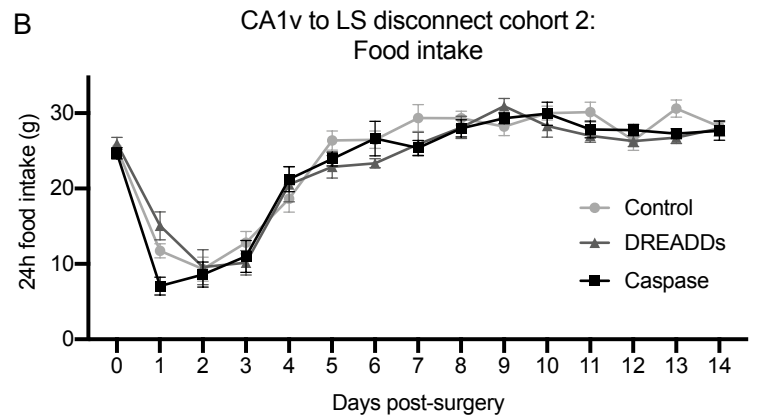Food intake
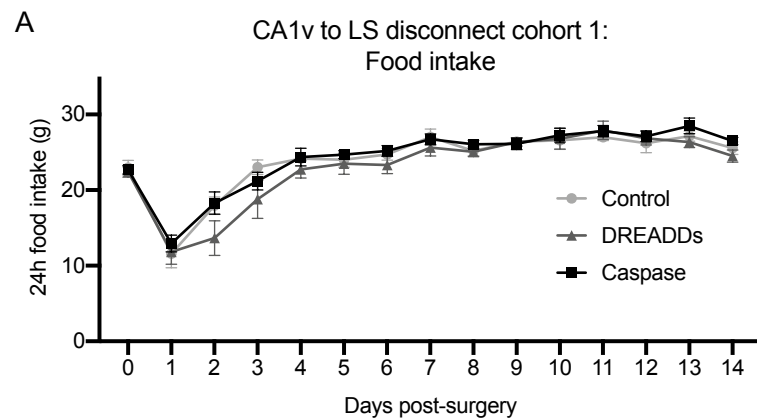
B

HPCv lesion:
Body weight

889   **Supplementary Figure 1. Effect of bilateral HPCv lesions on food intake and body weight.**

890   There were no effects on food intake (A) or body weight (B) of bilateral HPCv lesions compared

891   to controls. Lesion n = 11, control n = 18. All values expressed as mean +/- SEM.

892

893

Supplemental Figure 2

A — CA1v to LS disconnect cohort 1: Food intake

B — CA1v to LS disconnect cohort 2: Food intake

C — CA1v to LS disconnect cohort 1: Body weight

D — CA1v to LS disconnect cohort 2: Body weight

E — Cre-dependent tdTomato (Control)

F — Cre-dependent tdTomato (CA1v->LS caspase)

894 **Supplementary Figure 2. Effect of reversible and chronic disconnection of the CA1v to LS**

895 **neural pathway on food intake and body weight, and verification of the chronic approach.**

896 There were no effects on food intake (cohort 1: A; cohort 2: B) or body weight (cohort 1: C;

897 cohort 2: D) of reversible (DREADDs) or chronic (caspase) disconnection of the CA1v to LS

898 neural pathway compared to controls. Histological verification of the dual viral approach

899 demonstrates that cre-dependent tdTomato labeling of CA1v neurons induced by LS-origin retro-

900 cre is robust in a control animal (E), but reduced in an animal injected with cre-dependent

901 caspase combined with cre-dependent tdTomato due to caspase-induced cell death (F). For

902 graphs S1A-B (CA1v to LS disconnect cohort 1), DREADDs n=6, caspase n=10, control n=8.

903 For graphs S1C-D (CA1v to LS disconnect cohort 2), DREADDs n=8, caspase n=12, control
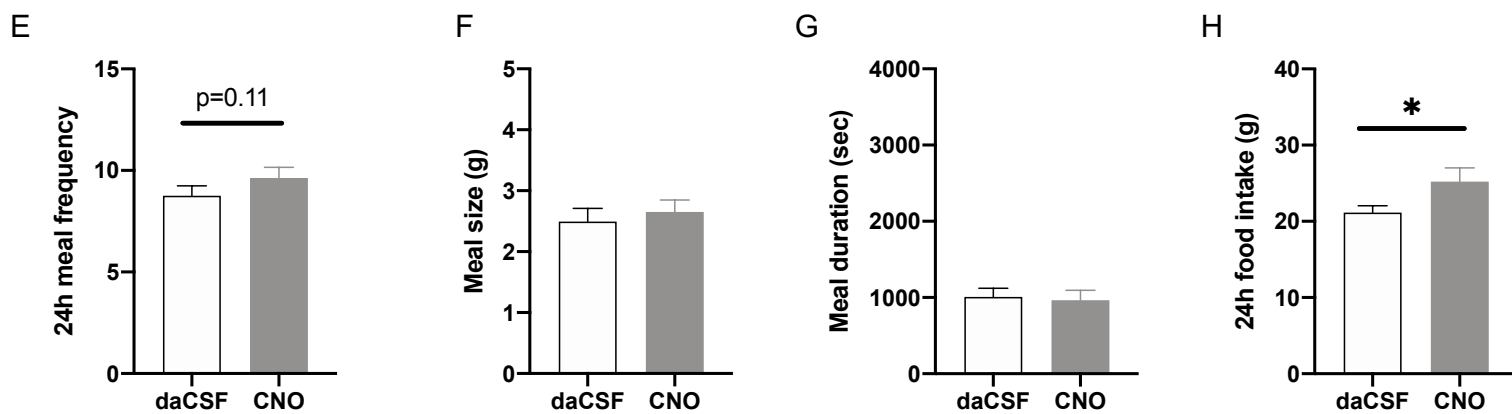
904 n=10. All values expressed as mean +/- SEM.

905

Supplemental Figure 3

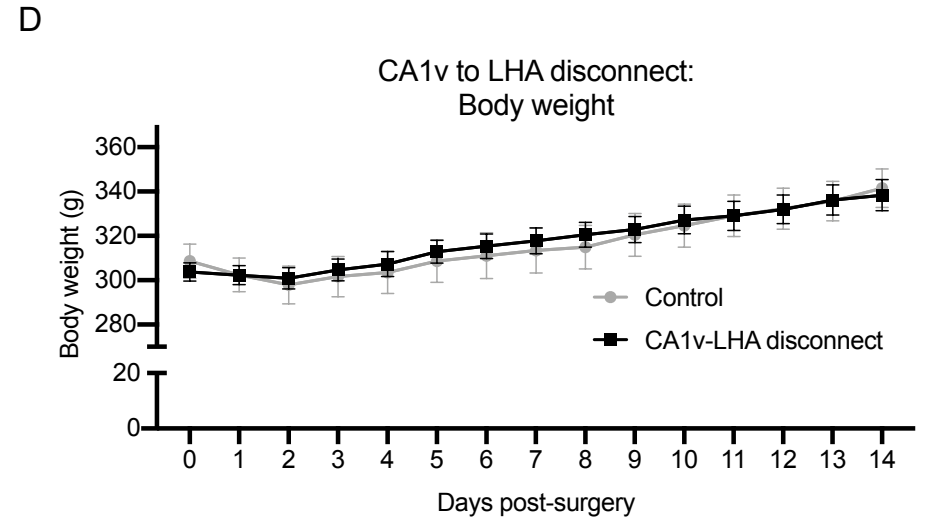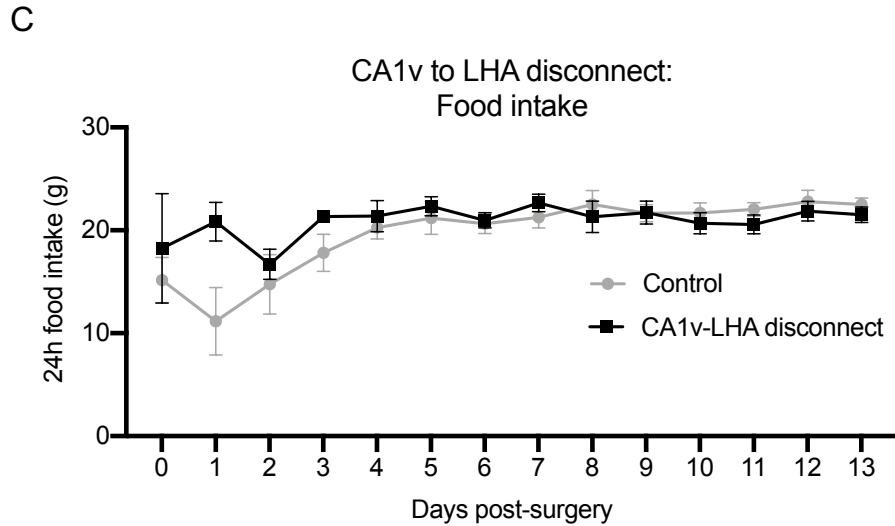## Chronic Disconnection of the vCA1-LS Pathway

A

B

C

D
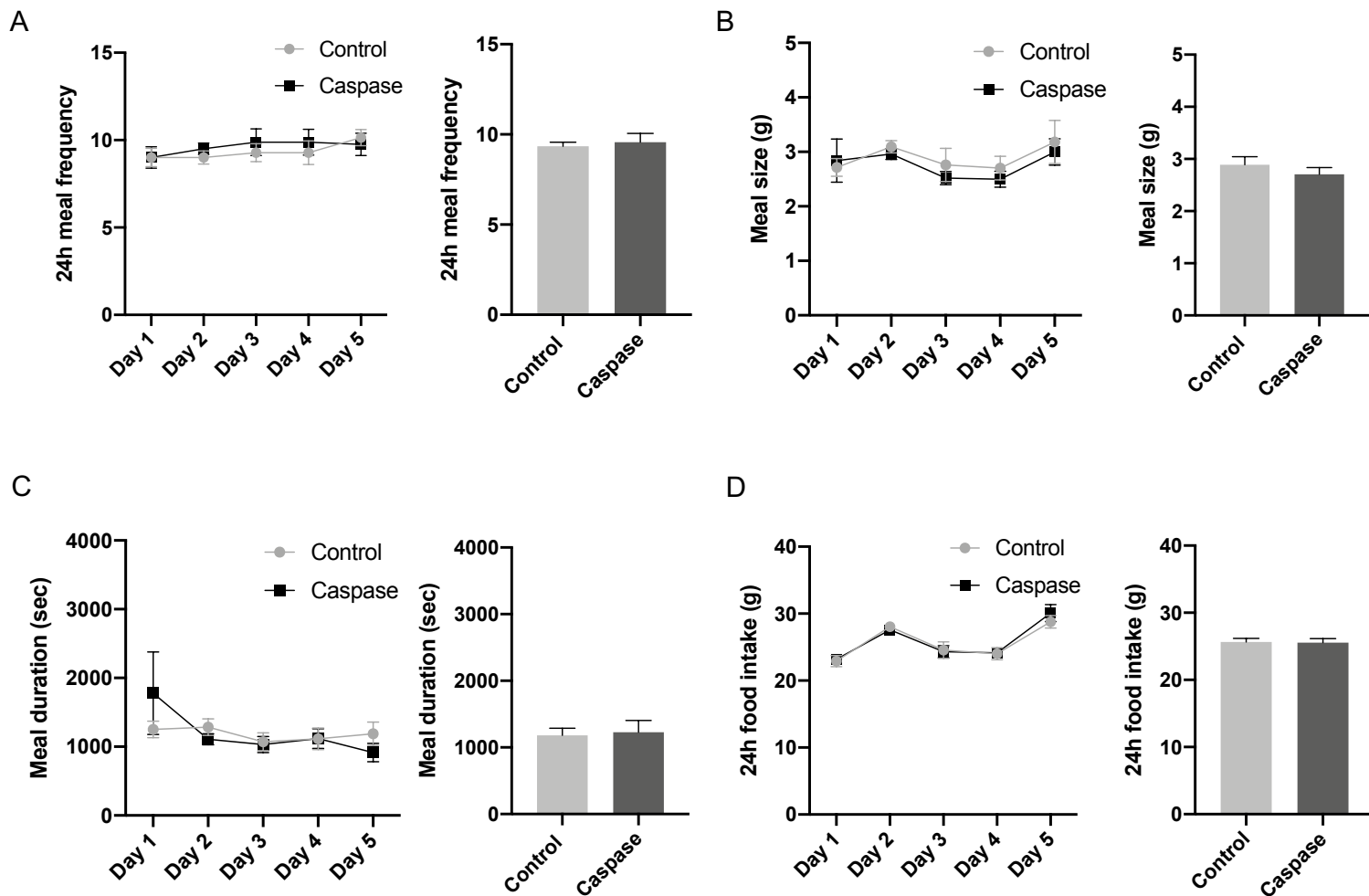
Acute Disconnection of the vCA1-LS Pathway

E

F

G

H

906 **Supplementary Figure 3. Effect of reversible and chronic disconnection of CA1v to LS**

907 **neural pathway on feeding behavior.** Compared with control animals, chronic caspase-

908 mediated disconnection of the CA1v to LS pathway did not significantly affect meal frequency

909 (A), meal size (B), meal duration (C), or 24h cumulative food intake (D) over the course of the

910 5-day recording period. Acute DREADDs-mediated disconnection of the CA1v to LS pathway

911 (via CNO infusion) resulted in non-significant trend towards increased meal frequency (E), no

912 differences in meal size (F) or meal duration (G), and a significant increase in 24h cumulative

913 food intake (H) in comparison with vehicle injection. All values expressed as mean +/- SEM.

914

Supplemental Figure 4

A

CA1v to mPFC disconnect:
Food intake

B

CA1v to mPFC disconnect:
Body weight

C

CA1v to LHA disconnect:
Food intake

D

CA1v to LHA disconnect:
Body weight
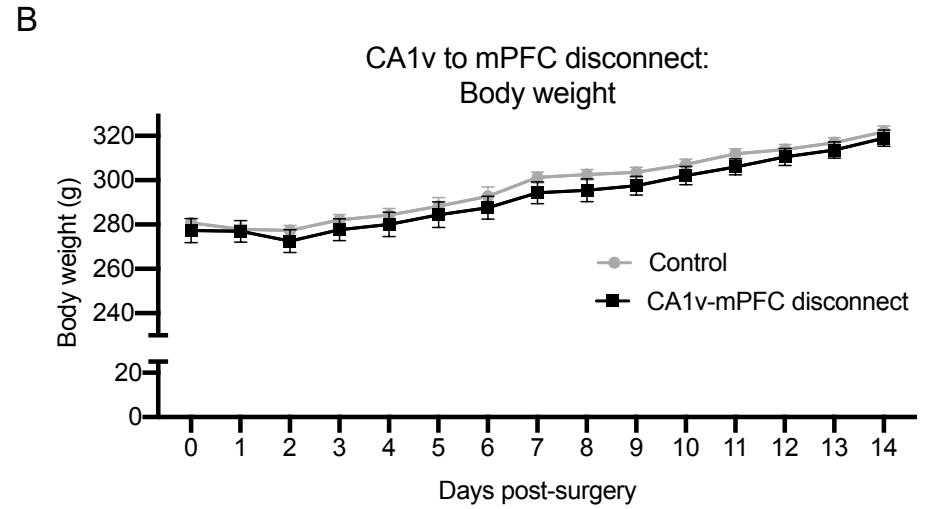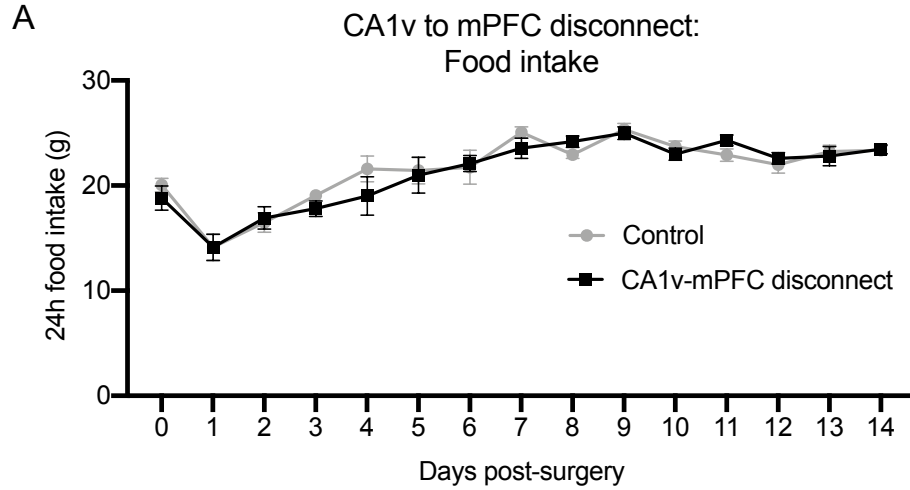
915 **Supplementary Figure 4. Effect of contralesional disconnection methods on food intake and**

916 **body weight.** There were no effects on food intake (A) or body weight (B) of contralesional

917 CA1v to mPFC compared to controls. CA1v to mPFC disconnect n=12, control n=12. There

918 were no effects on food intake (C) or body weight (D) of contralesional CA1v to LHA compared

919 to controls. CA1v to LHA disconnect n=12, control n=11. All values expressed as mean +/-

920 SEM.

921

922

928   **REFERENCES**

929

930   1.   R. D'Hooge, P. P. De Deyn, Applications of the Morris water maze in the study of
931   learning and memory. *Brain Res Brain Res Rev* **36**, 60-90 (2001).
932   2.   K. Gawel, E. Gibula, M. Marszalek-Grabska, J. Filarowska, J. H. Kotlinska, Assessment of
933   spatial learning and memory in the Barnes maze task in rodents-methodological
934   consideration. *Naunyn Schmiedebergs Arch Pharmacol* **392**, 1-18 (2019).
935   3.   R. G. M. Morris, U. Frey, "Hippocampal synaptic plasticity: Role in spatial learning or the
936   automatic recording of attended experience?" in Burgess, Neil (Ed); Jeffery, Kathryn J
937   (Ed); et al (1999) The hippocampal and parietal foundations of spatial cognition. (Oxford
938   University Press, U Edinburgh, Ctr for Neuroscience, Edinburgh, Scotland London, 1999),
939   pp. 220-246.
940   4.   D. C. Rowland, Y. Roudi, M. B. Moser, E. I. Moser, Ten Years of Grid Cells. *Annu Rev*
941   *Neurosci* **39**, 19-40 (2016).
942   5.   R. Morris, Developments of a water-maze procedure for studying spatial learning in the
943   rat. *Journal of neuroscience methods* **11**, 47-60 (1984).
944   6.   C. A. Barnes, Memory deficits associated with senescence: a neurophysiological and
945   behavioral study in the rat. *J Comp Physiol Psychol* **93**, 74-104 (1979).
946   7.   J. O'Keefe, J. Dostrovsky, The hippocampus as a spatial map: preliminary evidence from
947   unit activity in the freely-moving rat. *Brain research* (1971).
948   8.   T. Hafting, M. Fyhn, S. Molden, M. B. Moser, E. I. Moser, Microstructure of a spatial map
949   in the entorhinal cortex. *Nature* **436**, 801-806 (2005).
950   9.   M. S. Fanselow, H.-W. Dong, Are the dorsal and ventral hippocampus functionally
951   distinct structures? *Neuron* **65**, 7-19 (2010).
952   10.   A. T. Keinath *et al.*, Precise spatial coding is preserved along the longitudinal
953   hippocampal axis. *Hippocampus* **24**, 1533-1548 (2014).
954   11.   K. B. Kjelstrup *et al.*, Finite scale of spatial representation in the hippocampus. *Science*
955   **321**, 140-143 (2008).
956   12.   L. de Hoz, J. Knox, R. G. Morris, Longitudinal axis of the hippocampus: both septal and
957   temporal poles of the hippocampus support water maze spatial learning depending on
958   the training protocol. *Hippocampus* **13**, 587-603 (2003).
959   13.   J. Ferbinteanu, C. Ray, R. J. McDonald, Both dorsal and ventral hippocampus contribute
960   to spatial learning in Long-Evans rats. *Neurosci Lett* **345**, 131-135 (2003).
961   14.   M. B. Moser, E. I. Moser, Functional differentiation in the hippocampus. *Hippocampus* **8**,
962   608-619 (1998).
963   15.   S. E. Kanoski, H. J. Grill, Hippocampus Contributions to Food Intake Control: Mnemonic,
964   Neuroanatomical, and Endocrine Mechanisms. *Biol Psychiatry* **81**, 748-756 (2017).
965   16.   P. G. Henke, Hippocampal pathway to the amygdala and stress ulcer development. *Brain*
966   *Res Bull* **25**, 691-695 (1990).
967   17.   K. G. Kjelstrup *et al.*, Reduced fear expression after lesions of the ventral hippocampus.
968   *Proceedings of the National Academy of Sciences* **99**, 10825-10830 (2002).

969   18.   S. Gaskin, A. Gamliel, M. Tardif, E. Cole, D. G. Mumby, Incidental (unreinforced) and
970   reinforced spatial learning in rats with ventral and dorsal lesions of the hippocampus.
971   *Behav Brain Res* **202**, 64-70 (2009).
972   19.   M. S. Bienkowski *et al.*, Integration of gene expression and brain-wide connectivity
973   reveals the multiscale organization of mouse hippocampal networks. *Nat Neurosci* **21**,
974   1628-1643 (2018).
975   20.   R. Hannapel *et al.*, Postmeal Optogenetic Inhibition of Dorsal or Ventral Hippocampal
976   Pyramidal Neurons Increases Future Intake. *eNeuro* **6** (2019).
977   21.   R. C. Hannapel, Y. H. Henderson, R. Nalloor, A. Vazdarjanova, M. B. Parent, Ventral
978   hippocampal neurons inhibit postprandial energy intake. *Hippocampus* **27**, 274-284
979   (2017).
980   22.   B. K. Mani *et al.*, Neuroanatomical characterization of a growth hormone secretagogue
981   receptor-green fluorescent protein reporter mouse. *J Comp Neurol* **522**, 3644-3666
982   (2014).
983   23.   J. M. Zigman, J. E. Jones, C. E. Lee, C. B. Saper, J. K. Elmquist, Expression of ghrelin
984   receptor mRNA in the rat and the mouse brain. *J Comp Neurol* **494**, 528-548 (2006).
985   24.   I. Merchenthaler, M. Lane, P. Shughrue, Distribution of pre-pro-glucagon and glucagon-
986   like peptide-1 receptor messenger RNAs in the rat central nervous system. *J Comp
987   Neurol* **403**, 261-280 (1999).
988   25.   S. E. Kanoski, S. M. Fortin, K. M. Ricks, H. J. Grill, Ghrelin signaling in the ventral
989   hippocampus stimulates learned and motivational aspects of feeding via PI3K-Akt
990   signaling. *Biol Psychiatry* **73**, 915-923 (2013).
991   26.   S. E. Kanoski *et al.*, Hippocampal leptin signaling reduces food intake and modulates
992   food-related memory processing. *Neuropsychopharmacology* **36**, 1859-1870 (2011).
993   27.   T. M. Hsu *et al.*, A hippocampus to prefrontal cortex neural pathway inhibits food
994   motivation through glucagon-like peptide-1 signaling. *Mol Psychiatry* **23**, 1555-1565
995   (2018).
996   28.   T. M. Hsu, J. D. Hahn, V. R. Konanur, A. Lam, S. E. Kanoski, Hippocampal GLP-1 receptors
997   influence food intake, meal size, and effort-based responding for food through volume
998   transmission. *Neuropsychopharmacology* **40**, 327-337 (2015).
999   29.   A. N. Suarez, C. M. Liu, A. M. Cortella, E. E. Noble, S. E. Kanoski, Ghrelin and Orexin
1000   Interact to Increase Meal Size Through a Descending Hippocampus to Hindbrain
1001   Signaling Pathway. *Biol Psychiatry* **87**, 1001-1011 (2020).
1002   30.   G. D. Petrovich, N. S. Canteras, L. W. Swanson, Combinatorial amygdalar inputs to
1003   hippocampal domains and hypothalamic behavior systems. *Brain research reviews* **38**,
1004   247-289 (2001).
1005   31.   C. De La Rosa-Prieto *et al.*, Subicular and CA1 hippocampal projections to the accessory
1006   olfactory bulb. *Hippocampus* **19**, 124-129 (2009).
1007   32.   T. M. Hsu *et al.*, Hippocampus ghrelin receptor signaling promotes socially-mediated
1008   learned food preference. *Neuropharmacology* **131**, 487-496 (2018).
1009   33.   L. W. Swanson, W. M. Cowan, An autoradiographic study of the organization of the
1010   efferent connections of the hippocampal formation in the rat. *J Comp Neurol* **172**, 49-84
1011   (1977).

1012 34. T. M. Hsu *et al.*, Hippocampus ghrelin signaling mediates appetite through lateral
1013   hypothalamic orexin pathways. *Elife* **4** (2015).
1014 35. A. Arszovszki, Z. Borhegyi, T. Klausberger, Three axonal projection routes of individual
1015   pyramidal cells in the ventral CA1 hippocampus. *Front Neuroanat* **8**, 53 (2014).
1016 36. P. Y. Risold, L. W. Swanson, Structural evidence for functional domains in the rat
1017   hippocampus. *Science (New York, N.Y.)* **272**, 1484-1486 (1996).
1018 37. P. Sweeney, Y. Yang, An excitatory ventral hippocampus to lateral septum circuit that
1019   suppresses feeding. *Nat Commun* **6**, 10188 (2015).
1020 38. R. Garcia, R. M. Vouimba, R. Jaffard, Spatial discrimination learning induces LTP-like
1021   changes in the lateral septum of mice. *Neuroreport: An International Journal for the
1022   Rapid Communication of Research in Neuroscience* **5**, 329-332 (1993).
1023 39. R. Jaffard, R. M. Vouimba, A. Marighetto, R. Garcia, Long-term potentiation and long-
1024   term depression in the lateral septum in spatial working and reference memory. *J
1025   Physiol Paris* **90**, 339-341 (1996).
1026 40. S. J. Terrill *et al.*, Nucleus accumbens melanin-concentrating hormone signaling
1027   promotes feeding in a sex-specific manner. *Neuropharmacology* **178**, 108270 (2020).
1028 41. A. Carballo-Marquez, A. Vale-Martinez, G. Guillazo-Blanch, M. Marti-Nicolovius,
1029   Muscarinic receptor blockade in ventral hippocampus and prelimbic cortex impairs
1030   memory for socially transmitted food preference. *Hippocampus* **19**, 446-455 (2009).
1031 42. R. A. Countryman, N. L. Kaban, P. J. Colombo, Hippocampal c-fos is necessary for long-
1032   term memory of a socially transmitted food preference. *Neurobiol Learn Mem* **84**, 175-
1033   183 (2005).
1034 43. G. M. Parfitt *et al.*, Bidirectional Control of Anxiety-Related Behaviors in Mice: Role of
1035   Inputs Arising from the Ventral Hippocampus to the Lateral Septum and Medial
1036   Prefrontal Cortex. *Neuropsychopharmacology : official publication of the American
1037   College of Neuropsychopharmacology* **42**, 1715-1728 (2017).
1038 44. N. L. Trent, J. L. Menard, The ventral hippocampus and the lateral septum work in
1039   tandem to regulate rats' open-arm exploration in the elevated plus-maze. *Physiology &
1040   behavior* **101**, 141-152 (2010).
1041 45. J. C. Jimenez *et al.*, Anxiety Cells in a Hippocampal-Hypothalamic Circuit. *Neuron* **97**,
1042   670-683.e676 (2018).
1043 46. M. S. Fanselow, H. W. Dong, Are the dorsal and ventral hippocampus functionally
1044   distinct structures? *Neuron* **65**, 7-19 (2010).
1045 47. M. Contreras, T. Pelc, M. Llofriu, A. Weitzenfeld, J. M. Fellous, The ventral hippocampus
1046   is involved in multi-goal obstacle-rich spatial navigation. *Hippocampus* **28**, 853-866
1047   (2018).
1048 48. S. L. T. Lee, D. Lew, V. Wickenheisser, E. J. Markus, Interdependence between dorsal and
1049   ventral hippocampus during spatial navigation. *Brain Behav* **9**, e01410 (2019).
1050 49. D. P. Holschneider *et al.*, Cerebral perfusion mapping during retrieval of spatial memory
1051   in rats. *Behavioural brain research* **375**, 112116 (2019).
1052 50. D. Olivo, M. Caba, F. Gonzalez-Lima, J. F. Rodríguez-Landa, A. A. Corona-Morales,
1053   Metabolic activation of amygdala, lateral septum and accumbens circuits during food
1054   anticipatory behavior. *Behav Brain Res* **316**, 261-270 (2017).

1055 51. M. Carus-Cadavieco *et al.*, Gamma oscillations organize top-down signalling to
1056   hypothalamus and enable food seeking. *Nature* **542**, 232-236 (2017).
1057 52. S. J. Terrill *et al.*, Role of lateral septum glucagon-like peptide 1 receptors in food intake.
1058   *American journal of physiology. Regulatory, integrative and comparative physiology* **311**,
1059   R124-132 (2016).
1060 53. S. J. Terrill, K. D. Wall, N. D. Medina, C. B. Maske, D. L. Williams, Lateral septum growth
1061   hormone secretagogue receptor affects food intake and motivation for sucrose
1062   reinforcement. *American journal of physiology. Regulatory, integrative and comparative*
1063   *physiology* **315**, R76-r83 (2018).
1064 54. C. Wang, C. M. Kotz, Urocortin in the lateral septal area modulates feeding induced by
1065   orexin A in the lateral hypothalamus. *American journal of physiology. Regulatory,*
1066   *integrative and comparative physiology* **283**, R358-367 (2002).
1067 55. J. Hauser, L. H. Llano López, J. Feldon, P. A. Gargiulo, B. K. Yee, Small lesions of the dorsal
1068   or ventral hippocampus subregions are associated with distinct impairments in working
1069   memory and reference memory retrieval, and combining them attenuates the
1070   acquisition rate of spatial reference memory. *Hippocampus* **30**, 938-957 (2020).
1071 56. D. S. Olton, The radial arm maze as a tool in behavioral pharmacology. *Physiology &*
1072   *behavior* **40**, 793-797 (1987).
1073 57. H. H. Pothuizen, W. N. Zhang, A. L. Jongen-Rêlo, J. Feldon, B. K. Yee, Dissociation of
1074   function between the dorsal and the ventral hippocampus in spatial learning abilities of
1075   the rat: a within-subject, within-task comparison of reference and working spatial
1076   memory. *The European journal of neuroscience* **19**, 705-712 (2004).
1077 58. L. E. Jarrard, L. P. Luu, T. L. Davidson, A study of hippocampal structure-function
1078   relations along the septo-temporal axis. *Hippocampus* **22**, 680-692 (2012).
1079 59. L. W. Swanson, Brain maps 4.0-Structure of the rat brain: An open access atlas with
1080   global nervous system nomenclature ontology and flatmaps. *J Comp Neurol* **526**, 935-
1081   943 (2018).
1082 60. R. C. Ritter, P. G. Slusser, S. Stone, Glucoreceptors controlling feeding and blood glucose:
1083   location in the hindbrain. *Science* **213**, 451-452 (1981).
1084 61. E. E. Noble *et al.*, Hypothalamus-hippocampus circuitry regulates impulsivity via
1085   melanin-concentrating hormone. *Nat Commun* **10**, 4923 (2019).
1086 62. B. Zingg *et al.*, AAV-Mediated Anterograde Transsynaptic Tagging: Mapping
1087   Corticocollicular Input-Defined Neural Pathways for Defense Behaviors. *Neuron* **93**, 33-
1088   47 (2017).
1089 63. A. N. Suarez *et al.*, Gut vagal sensory signaling regulates hippocampus function through
1090   multi-order pathways. *Nat Commun* **9**, 2181 (2018).
1091 64. J. D. Hahn, O. Sporns, A. G. Watts, L. W. Swanson, Macroscale intrinsic network
1092   architecture of the hypothalamus. *Proc Natl Acad Sci U S A* **116**, 8018-8027 (2019).
1093 65. J. D. Hahn, Swanson, L. W,. Bowman, I., Foster, N. N., Zingg, B., Bienkowski, M. S.,
1094   Hintiryan, H., & Dong, H.-W. , An open access mouse brain flatmap and upgraded rat
1095   and human brain flatmaps based on current reference atlases. *J. Comp. Neurol.* (2020).
1096 66. L. E. Herzog *et al.*, Interaction of Taste and Place Coding in the Hippocampus. *The*
1097   *Journal of neuroscience : the official journal of the Society for Neuroscience* **39**, 3057-
1098   3069 (2019).

1099   67.   R. A. Countryman, P. E. Gold, Rapid forgetting of social transmission of food preferences
1100   in aged rats: relationship to hippocampal CREB activation. *Learn Mem* **14**, 350-358
1101   (2007).
1102   68.   B. G. Galef, Jr., W. Y. Lee, E. E. Whiskin, Lack of interference in long-term memory for
1103   socially learned food preferences in rats (Rattus norvegicus). *J Comp Psychol* **119**, 131-
1104   135 (2005).
1105   69.   B. G. Galef, Jr., E. E. Whiskin, Socially transmitted food preferences can be used to study
1106   long-term memory in rats. *Learn Behav* **31**, 160-164 (2003).
1107